

# Learning Mixture Density via Natural Gradient Expectation Maximization

Yutao Chen<sup>1</sup> Jasmine Bayrooti<sup>2</sup> Steven Morad<sup>1</sup>

## Abstract

Mixture density networks are neural networks that produce Gaussian mixtures to represent continuous multimodal conditional densities. Standard training procedures involve maximum likelihood estimation using the negative log-likelihood (NLL) objective, which suffers from slow convergence and mode collapse. In this work, we improve the optimization of mixture density networks by integrating their information geometry. Specifically, we interpret mixture density networks as deep latent-variable models and analyze them through an expectation maximization framework, which reveals surprising theoretical connections to natural gradient descent. We exploit such connections to derive the natural gradient expectation maximization (nGEM) objective. We empirically show that nGEM achieves up to  $10\times$  faster convergence while adding almost *zero* computational overhead, and scales well to high-dimensional data where NLL otherwise fails.

## 1. Introduction

Predictive modeling is a central task in probabilistic machine learning, where one posits a conditional distribution  $p(\mathbf{y}|\mathbf{x})$  over the features  $\mathbf{x}$  and targets  $\mathbf{y}$ . For cases where  $\mathbf{y}$  is continuous, it is usually analytically convenient to assume that  $p(\mathbf{y}|\mathbf{x})$  is Gaussian. However, Gaussian distributions are unimodal and hence incapable of fitting *multimodal* distributions. An alternative is the Gaussian mixture model, which approximates arbitrary continuous smooth densities via a finite convex combination of Gaussian components.

Building upon Gaussian mixtures, mixture density networks (Bishop, 1994) constitute a family of flexible probabilistic models designed for fitting complex and multimodal conditional distributions. Specifically, mixture density networks leverage neural networks to map features  $\mathbf{x}$  to the distributional parameters of Gaussian mixtures that approximate the

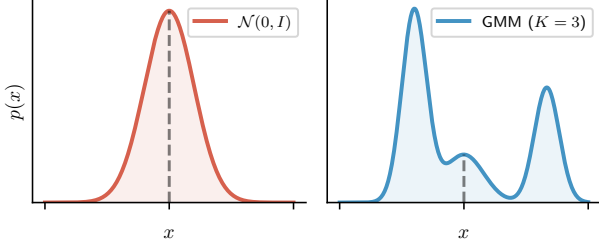


Figure 1. (Left) A standard Gaussian distribution compared with (right) a multimodal Gaussian mixture model. Both share the same mean  $\mathbb{E}[x] = 0$  while the Gaussian mixture is more flexible.

conditional density  $p(\mathbf{y}|\mathbf{x})$ . Mixture density networks are conventionally optimized via stochastic gradient descent by minimizing the negative log-likelihood loss (Bishop, 1994).

Mixture density networks are widely used for uncertainty-aware prediction and multi-valued regression, where an input  $\mathbf{x}$  may correspond to multiple valid outputs  $\mathbf{y}$ , e.g., speech synthesis (Capes et al., 2017), inverse kinematics or forward dynamics (Ha & Schmidhuber, 2018) in robotics. However, despite being accessible in principle, the optimization of mixture density networks is often challenging, impeding practical adoption. Particularly, the loss landscape of Gaussian mixture negative log-likelihood is non-convex and contains many poor local minima (Chen et al., 2024). Empirical studies (Li & Lee, 2019; Makansi et al., 2019) also reveal that mixture density networks are susceptible to training inefficiency and mode collapse, where Gaussian mixtures effectively degenerate into one singular Gaussian.

**Our Contributions** We revisit mixture density network optimization through the lens of latent-variable models and expectation maximization (EM). We identify theoretical connections between EM and natural gradient descent for Gaussian mixtures, and exploit such connections to construct a tractable natural gradient EM (nGEM) objective that yields fast and stable convergence by leveraging the information geometry of the underlying probabilistic models.

Empirically, we demonstrate that nGEM effectively stabilizes and accelerates mixture density network optimization, achieving up to  $10\times$  faster convergence with negligible extra computational overhead. We further validate the scalability of nGEM with high-dimensional and practical datasets.

<sup>1</sup>Faculty of Science and Technology, University of Macau

<sup>2</sup>University of Cambridge. Correspondence to: Steven Morad <smorad@um.edu.mo>.

## 2. Preliminaries

In this section, we briefly review the foundational concepts: **mixture density networks** (MDNs), **natural gradient descent** (NGD), and **expectation maximization** (EM), upon which the proposed method nGEM is established.

**Mixture Density Networks** (MDNs) (Bishop, 1994) model flexible conditional distributions  $p(\mathbf{y}|\mathbf{x})$  using Gaussian mixtures and neural networks. Specifically, MDNs learn a neural network  $f(\mathbf{x}; \boldsymbol{\theta})$  parametrized by  $\boldsymbol{\theta}$  that maps conditions  $\mathbf{x}$  to the parameters  $\phi^{(\mathbf{x})}$  of a Gaussian mixture, where

$$\phi^{(\mathbf{x})} = \{\pi_k^{(\mathbf{x})}, \boldsymbol{\mu}_k^{(\mathbf{x})}, \boldsymbol{\Sigma}_k^{(\mathbf{x})}\}_{k=1}^K \quad (1)$$

is the collection of the weights<sup>1</sup>, means, and covariances of the  $K$  Gaussian mixture components conditioned on  $\mathbf{x}$ . The conditional distribution  $p(\mathbf{y}|\mathbf{x})$  is thus

$$p(\mathbf{y}|\mathbf{x}) = \sum_{k=1}^K \pi_k^{(\mathbf{x})} \mathcal{N}(\mathbf{y}; \boldsymbol{\mu}_k^{(\mathbf{x})}, \boldsymbol{\Sigma}_k^{(\mathbf{x})}). \quad (2)$$

Given data points  $\{\mathbf{x}, \mathbf{y}\}$ , the parameters  $\boldsymbol{\theta}$  are optimized typically by minimizing the negative log-likelihood (NLL)

$$\mathcal{L}_{\text{NLL}}(\boldsymbol{\theta}) = -\log \sum_{k=1}^K \pi_k^{(\mathbf{x})} \mathcal{N}(\mathbf{y}; \boldsymbol{\mu}_k^{(\mathbf{x})}, \boldsymbol{\Sigma}_k^{(\mathbf{x})}). \quad (3)$$

**Natural Gradient Descent** (NGD) (Amari, 1998) is a generalization of the canonical gradient descent (GD) algorithm that accounts for the curvature of the parameter space of probabilistic models  $p(\mathbf{x}|\boldsymbol{\theta})$ . Consider minimizing the objective  $J(\boldsymbol{\theta})$  with a learning rate  $\beta$  via gradient descent

$$\boldsymbol{\theta}_{t+1} \leftarrow \boldsymbol{\theta}_t - \beta \nabla J(\boldsymbol{\theta}_t). \quad (4)$$

GD performs steepest descent with a Euclidean distance penalty between parameter updates  $\|\boldsymbol{\theta}_t - \boldsymbol{\theta}_{t+1}\|_2^2$ . For probabilistic models  $p(\mathbf{x}|\boldsymbol{\theta})$ , however, a more *natural* penalty<sup>2</sup> is the KL divergence  $\mathbb{D}_{\text{KL}}(p(\mathbf{x}|\boldsymbol{\theta}_t) \| p(\mathbf{x}|\boldsymbol{\theta}_{t+1}))$  between the induced distributions, which leads to the NGD update:

$$\boldsymbol{\theta}_{t+1} \leftarrow \boldsymbol{\theta}_t - \beta F^{-1}(\boldsymbol{\theta}_t) \nabla J(\boldsymbol{\theta}_t), \quad (5)$$

where  $F^{-1}(\boldsymbol{\theta}_t)$  is the inverse of the *Fisher information matrix* (FIM) of  $p(\mathbf{x}|\boldsymbol{\theta}_t)$ . Specifically, the FIM  $F(\boldsymbol{\theta})$ , under certain conditions (Martens, 2020, Section 5), can be defined as the negative expected Hessian of the log density

$$F(\boldsymbol{\theta}) = -\mathbb{E}_{p(\mathbf{x}|\boldsymbol{\theta})} [\nabla_{\boldsymbol{\theta}}^2 \log p(\mathbf{x}|\boldsymbol{\theta})]. \quad (6)$$

Intuitively, NGD utilizes second-order derivatives (FIM) to capture the local geometry of probabilistic models, re-projecting the gradient updates appropriately for faster and

more stable optimization. However, a critical downside of NGD lies in the computation and inversion of the FIM  $F(\boldsymbol{\theta})$ , which in many cases are intractable and require expensive approximation (Martens, 2020).

**Expectation Maximization** (EM) (Dempster et al., 1977) is an algorithm for finding maximum likelihood solutions of probabilistic models with missing data. EM is particularly well-known for its application in Gaussian mixture models, where each observed data point is assumed to be generated by one of the mixture components whose identity is missing.

Let  $\mathbf{x}$  denote the observed data,  $\mathbf{z}$  denote the missing data, and  $p(\mathbf{x}, \mathbf{z}|\boldsymbol{\theta})$  denote the probabilistic model parametrized by  $\boldsymbol{\theta}$ . Directly maximizing the observed-data log-likelihood  $\log p(\mathbf{x}|\boldsymbol{\theta}) = \log \int p(\mathbf{x}, \mathbf{z}|\boldsymbol{\theta}) d\mathbf{z}$  is generally difficult due to the integration over  $\mathbf{z}$ . However, note that

$$\log p(\mathbf{x}|\boldsymbol{\theta}) = \mathcal{F}(q(\mathbf{z}), \boldsymbol{\theta}) + \mathbb{D}_{\text{KL}}(q(\mathbf{z}) \| p(\mathbf{z}|\mathbf{x}; \boldsymbol{\theta})), \quad (7)$$

where

$$\mathcal{F}(q(\mathbf{z}), \boldsymbol{\theta}) = \mathbb{E}_{q(\mathbf{z})} \left[ \log \frac{p(\mathbf{x}, \mathbf{z}|\boldsymbol{\theta})}{q(\mathbf{z})} \right] \leq \log p(\mathbf{x}|\boldsymbol{\theta}) \quad (8)$$

is a lower bound of  $\log p(\mathbf{x}|\boldsymbol{\theta})$  (known as the *evidence lower bound*, or ELBO) since KL divergence is non-negative (Neal & Hinton, 1998).

The EM algorithm maximizes  $\log p(\mathbf{x}|\boldsymbol{\theta})$  by instead maximizing the lower bound  $\mathcal{F}(q(\mathbf{z}), \boldsymbol{\theta})$  iteratively. For each iteration  $t$ , we alternate between the E-step and the M-step:

- **(E-step)** we maximize  $\mathcal{F}(q(\mathbf{z}), \boldsymbol{\theta})$  with  $\boldsymbol{\theta} = \boldsymbol{\theta}_t$

$$q_t(\mathbf{z}) = \arg \max_{q(\mathbf{z})} \mathcal{F}(q(\mathbf{z}), \boldsymbol{\theta}_t) = p(\mathbf{z}|\mathbf{x}; \boldsymbol{\theta}_t). \quad (9)$$

- **(M-step)** we maximize  $\mathcal{F}(q(\mathbf{z}), \boldsymbol{\theta})$  with  $q(\mathbf{z}) = q_t(\mathbf{z})$

$$\begin{aligned} \boldsymbol{\theta}_{t+1} &= \arg \max_{\boldsymbol{\theta}} \mathcal{F}(q_t(\mathbf{z}), \boldsymbol{\theta}) \\ &= \arg \max_{\boldsymbol{\theta}} \int p(\mathbf{z}|\mathbf{x}; \boldsymbol{\theta}_t) \log p(\mathbf{x}, \mathbf{z}|\boldsymbol{\theta}) d\mathbf{z}. \end{aligned} \quad (10)$$

EM guarantees monotonic improvement of  $\log p(\mathbf{x}|\boldsymbol{\theta})$  until convergence to some *local* maxima (Dempster et al., 1977).

For cases where exact maximization is not tractable, the M-step can be substituted with gradient ascent steps, leading to the generalized EM (Bishop, 2006, Chapter 9) algorithm.

## 3. Natural Gradient EM

While Gaussian mixtures in theory are capable of approximating any continuous density (Bishop, 2006, Chapter 2), in practice mixture density networks are found to suffer from slow convergence and mode collapse (Li & Lee, 2019;

<sup>1</sup> The Gaussian mixture weights  $\boldsymbol{\pi}$  satisfies  $\boldsymbol{\pi} \in \Delta^{K-1}$ .

<sup>2</sup> We refer readers to Section A for full justification for NGD.

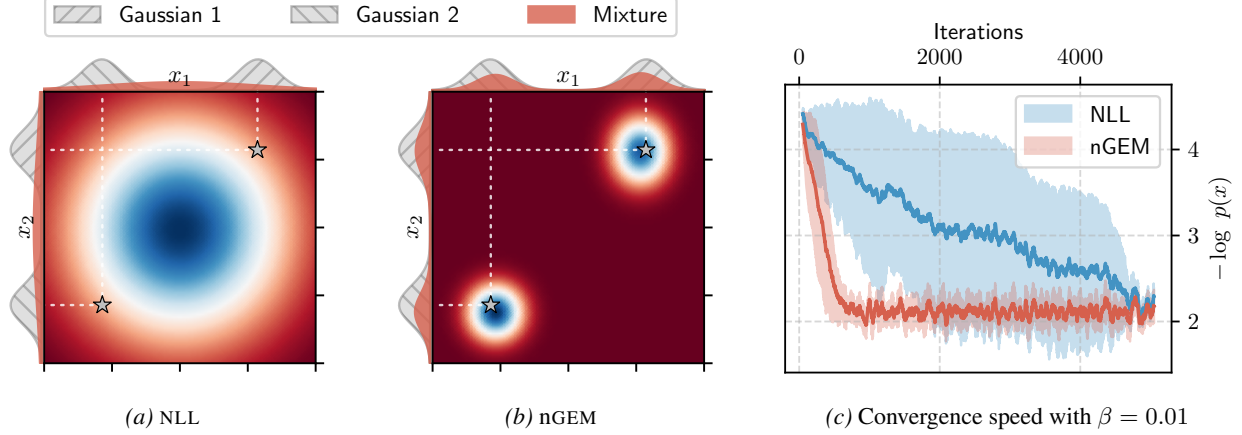


Figure 2. Fitting two Gaussians with a Gaussian mixture model (GMM) in  $\mathbb{R}^2$ . (a) Mode collapse using NLL loss. (b) Mode separation using nGEM loss. Heatmaps denote the probability density of the learned GMM, while stars ( $\star$ ) denote means of the ground truth Gaussians. Marginal distributions are also displayed with hashed gray regions representing the ground truth Gaussians and red regions representing the learned mixture density. (c) Negative log-likelihoods ( $\downarrow$ ) of GMMs with a learning rate  $\beta = 10^{-2}$ , averaged ( $\pm$  std) across 5 random seeds.

Makansi et al., 2019), where the model manages to locate a *subpar mean fit* using one mixture component to cover all or multiple modes in the target distribution (see Figure 2a).

One could consider improving the standard NLL objective using NGD, which accounts for the geometry of the parameter space. Unfortunately, this approach is not applicable directly as the FIM of Gaussian mixtures is non-analytical<sup>3</sup>.

To address this intractability, we propose natural gradient expectation maximization (nGEM). Building upon classic Gaussian mixture models, we establish an EM framework for learning mixture density (§3.1). We show that EM, NGD, and NLL for Gaussian mixtures are connected and in fact equivalent under mild assumptions (§3.2). We then exploit such connections to derive a *tractable* natural gradient EM (nGEM) algorithm for learning mixture density (§3.3).

### 3.1. Stochastic Gradient EM

We begin by reinterpreting mixture density networks as deep latent-variable models, with observed features  $\mathbf{x}$  and targets  $\mathbf{y}$ , latent variables  $\mathbf{z}$ , and network parameters  $\theta$ . The joint conditional distribution of  $\{\mathbf{y}, \mathbf{z}\}$  given  $\mathbf{x}$  is<sup>4</sup>

$$p(\mathbf{y}, \mathbf{z}|\mathbf{x}; \theta) = p(\mathbf{z}|\mathbf{x}; \theta)p(\mathbf{y}|\mathbf{x}, \mathbf{z}; \theta), \quad (11)$$

where  $p(\mathbf{z}|\mathbf{x})$  is a categorical distribution

$$p(\mathbf{z}|\mathbf{x}) = \text{Cat}(\pi_1^{(\mathbf{x})}, \pi_2^{(\mathbf{x})}, \dots, \pi_K^{(\mathbf{x})}), \quad (12)$$

and  $p(\mathbf{y}|\mathbf{x}, \mathbf{z})$  is a Gaussian distribution

$$p(\mathbf{y}|\mathbf{x}, \mathbf{z} = k) = \mathcal{N}(\mathbf{y}; \boldsymbol{\mu}_k^{(\mathbf{x})}, \boldsymbol{\Sigma}_k^{(\mathbf{x})}). \quad (13)$$

<sup>3</sup> We refer the readers to §B.5 for further justification.

<sup>4</sup> We shall omit  $\theta$  hereafter whenever there is no ambiguity.

We obtain the observed-data log-likelihood of MDNs by marginalizing  $p(\mathbf{y}, \mathbf{z}|\mathbf{x})$  over latent variables  $\mathbf{z}$ :

$$\log p(\mathbf{y}|\mathbf{x}) = \log \sum_{k=1}^K \pi_k^{(\mathbf{x})} \mathcal{N}(\mathbf{y}; \boldsymbol{\mu}_k^{(\mathbf{x})}, \boldsymbol{\Sigma}_k^{(\mathbf{x})}), \quad (14)$$

which coincides with the negative of  $\mathcal{L}_{\text{NLL}}$  (3). Recall that EM maximizes the observed-data log-likelihood (or equivalently minimizing NLL) by maximizing the lower bound objective  $\mathcal{F}(q(\mathbf{z}), \theta)$  (8). Similarly for MDNs, we follow an iterative EM process. In the **E-step**, we compute (9)

$$\begin{aligned} q_t(\mathbf{z} = k|\mathbf{x}) &= p(\mathbf{z} = k|\mathbf{x}, \mathbf{y}; \theta_t) \\ &= \frac{\pi_k^{(\mathbf{x})} \mathcal{N}(\mathbf{y}; \boldsymbol{\mu}_k^{(\mathbf{x})}, \boldsymbol{\Sigma}_k^{(\mathbf{x})})}{\sum_{j=1}^K \pi_j^{(\mathbf{x})} \mathcal{N}(\mathbf{y}; \boldsymbol{\mu}_j^{(\mathbf{x})}, \boldsymbol{\Sigma}_j^{(\mathbf{x})})}. \end{aligned} \quad (15)$$

For brevity, we let  $\rho_k^{(\mathbf{x})} = q_t(\mathbf{z} = k|\mathbf{x})$  where  $\rho^{(\mathbf{x})} \in \mathbb{R}^K$  is known as the *responsibilities*, explaining how much each mixture component is responsible for data points  $\{\mathbf{x}, \mathbf{y}\}$ .

In the **M-step**, however, we do not directly maximize w.r.t. the Gaussian mixture parameters  $\phi^{(\mathbf{x})}$  (1), but instead w.r.t. the parameters  $\theta$  of the neural network  $f(\mathbf{x}; \theta)$  that generates  $\phi^{(\mathbf{x})}$ . Exact maximization is generally intractable due to the complex and non-linear nature of neural networks.

Following the generalized EM algorithm, we opt for stochastic gradient descent to maximize the M-step objective (10), leading to the stochastic gradient EM (SGEM) loss

$$\begin{aligned} \mathcal{L}_{\text{SGEM}}(\theta) &= - \int p(\mathbf{z}|\mathbf{x}, \mathbf{y}; \theta_t) \log p(\mathbf{y}, \mathbf{z}|\mathbf{x}; \theta) d\mathbf{z} \\ &= - \sum_{k=1}^K \left[ \rho_k^{(\mathbf{x})} \right] \log \pi_k^{(\mathbf{x})} \mathcal{N}(\mathbf{y}; \boldsymbol{\mu}_k^{(\mathbf{x})}, \boldsymbol{\Sigma}_k^{(\mathbf{x})}), \end{aligned} \quad (16)$$

where  $\lfloor \cdot \rfloor$  is the *stop-gradient* operator preventing gradient backpropagation, as the responsibilities  $\rho^{(x)}$  from the E-step are held constant during the M-step as in canonical EM<sup>5</sup>.

### 3.2. Connecting EM and NGD

Intriguingly, we observe that in practice, the negative log-likelihood loss (3) and the stochastic gradient EM loss (16) always result in *identical* models under controlled random seeds. We can formalize this insight by proving that  $\nabla \mathcal{L}_{\text{NLL}}(\boldsymbol{\theta}) = \nabla \mathcal{L}_{\text{SGEM}}(\boldsymbol{\theta})$  as follows.

**Proposition 3.1** (Salakhutdinov et al., 2003; Xu et al., 2024). *Consider a probabilistic model  $p(\mathbf{x}, \mathbf{z}|\boldsymbol{\theta})$  with observed variables  $\mathbf{x}$ , latent variables  $\mathbf{z}$ , and parameters  $\boldsymbol{\theta}$ . We can show that*

$$\nabla_{\boldsymbol{\theta}} \log p(\mathbf{x}|\boldsymbol{\theta})|_{\boldsymbol{\theta}=\boldsymbol{\theta}_t} = \nabla_{\boldsymbol{\theta}} Q(\boldsymbol{\theta}|\boldsymbol{\theta}_t)|_{\boldsymbol{\theta}=\boldsymbol{\theta}_t},$$

where  $Q(\boldsymbol{\theta}|\boldsymbol{\theta}_t)$  is the M-step objective (10)

$$Q(\boldsymbol{\theta}|\boldsymbol{\theta}_t) = \int p(\mathbf{z}|\mathbf{x}; \boldsymbol{\theta}_t) \log p(\mathbf{x}, \mathbf{z}|\boldsymbol{\theta}) d\mathbf{z}.$$

*Proof.* See §B.1.  $\square$

Theorem 3.1 states that the gradient of the observed-data log-likelihood  $\log p(\mathbf{x}|\boldsymbol{\theta})$  is equal to the gradient of the M-step objective  $Q(\boldsymbol{\theta}|\boldsymbol{\theta}_t)$  at  $\boldsymbol{\theta} = \boldsymbol{\theta}_t$ . We can extend this conclusion to mixture density networks as follows.

**Corollary 3.2.** *Consider a mixture density network  $f(\mathbf{x}; \boldsymbol{\theta})$  parametrized by  $\boldsymbol{\theta}$ . We can show that*

$$\nabla_{\boldsymbol{\theta}} \mathcal{L}_{\text{NLL}}(\boldsymbol{\theta})|_{\boldsymbol{\theta}=\boldsymbol{\theta}_t} = \nabla_{\boldsymbol{\theta}} \mathcal{L}_{\text{SGEM}}(\boldsymbol{\theta})|_{\boldsymbol{\theta}=\boldsymbol{\theta}_t},$$

where  $\boldsymbol{\theta}_t$  is the parameter used for evaluating  $\rho^{(x)}$  (15).

*Proof.* See §B.2.  $\square$

Theorems 3.1 and 3.2 show that SGEM offers no additional benefits over NLL when only first-order optimizers (e.g. stochastic GD, Adam (Kingma & Ba, 2017)) are involved, as their gradients are equal.

However, SGEM unlocks an alternative view of NLL that allows bypassing the intractability of Gaussian mixture FIM and enables tractable natural gradient updates for MDNs. We start by showing that exact EM is equivalent to NGD.

**Proposition 3.3** (Sato, 2001). *For EM algorithms with exact E-M steps (9, 10), we show that the update  $\boldsymbol{\theta}_t \rightarrow \boldsymbol{\theta}_{t+1}$  is equivalent to a natural gradient descent step on the negative log-likelihood up to second-order Taylor approximation*

$$\boldsymbol{\theta}_{t+1} = \boldsymbol{\theta}_t - \hat{F}(\boldsymbol{\theta}_t)^{-1} \nabla_{\boldsymbol{\theta}} (-\log p(\mathbf{x}|\boldsymbol{\theta}_t)),$$

<sup>5</sup>Stochastic gradient EM admits a convenient factorized form that will later be useful for deriving natural gradient EM in §3.3.

where the learning rate is one, and  $\hat{F}(\boldsymbol{\theta}_t)$  is the complete-data Fisher information matrix at  $\boldsymbol{\theta} = \boldsymbol{\theta}_t$

$$\hat{F}(\boldsymbol{\theta}) = -\mathbb{E}_{p(\mathbf{x}, \mathbf{z}|\boldsymbol{\theta})} [\nabla_{\boldsymbol{\theta}}^2 \log p(\mathbf{x}, \mathbf{z}|\boldsymbol{\theta})].$$

*Proof.* See §B.3.  $\square$

For mixture density networks  $f(\mathbf{x}; \boldsymbol{\theta})$ , although exact EM updates are not possible, we can emulate such behaviors via natural gradient descent on the SGEM objective (16) using the *complete-data FIM*  $\hat{F}(\phi^{(x)})$  w.r.t. the Gaussian mixture parameters  $\phi^{(x)}$  (1):

$$\begin{aligned} \boldsymbol{\theta}_{t+1} &= \boldsymbol{\theta}_t - \hat{F}(\phi^{(x)})^{-1} \underbrace{\nabla_{\phi^{(x)}} \mathcal{L}_{\text{NLL}}(\boldsymbol{\theta}_t) \cdot \nabla_{\boldsymbol{\theta}} \phi^{(x)}}_{\text{Chain rule}}, \\ &= \boldsymbol{\theta}_t - \hat{F}(\phi^{(x)})^{-1} \underbrace{\nabla_{\phi^{(x)}} \mathcal{L}_{\text{SGEM}}(\boldsymbol{\theta}_t) \cdot \nabla_{\boldsymbol{\theta}} \phi^{(x)}}_{\text{Theorem 3.2}}. \end{aligned} \quad (17)$$

Furthermore, we can show that the complete-data FIM of Gaussian mixtures is block-diagonal, allowing independent natural gradient updates for each component distribution.

**Proposition 3.4.** *Consider a Gaussian mixture  $p(\mathbf{x}, \mathbf{z}|\boldsymbol{\theta})$  with observed variables  $\mathbf{x}$ , latent variables  $\mathbf{z}$ , and parameters  $\boldsymbol{\theta} = \{\pi_k, \boldsymbol{\mu}_k, \boldsymbol{\Sigma}_k\}_{k=1}^K$ . We can show that the complete-data FIM  $\hat{F}(\boldsymbol{\theta})$  of Gaussian mixtures is block-diagonal with  $K + 1$  blocks as shown below:*

$$\hat{F}(\boldsymbol{\theta}) = \begin{bmatrix} \pi_1 F_1 & \cdots & 0 & 0 \\ \vdots & \ddots & \vdots & \vdots \\ 0 & \cdots & \pi_K F_K & \vdots \\ 0 & \cdots & \cdots & F_{\pi} \end{bmatrix},$$

where  $F_k$  for  $k \in \{1, \dots, K\}$  is the FIM of the  $k$ -th Gaussian, and  $F_{\pi}$  is the FIM of the categorical distribution.

*Proof.* See §B.4.  $\square$

Theorem 3.4 and Equation (17) enable tractable natural gradient EM updates for MDNs, which we detail in §3.3.

**Summary** We prove that (a) SGEM is equivalent to NLL in gradients, and (b) exact EM is equivalent to NGD. We proceed to show that one can construct tractable natural gradient EM updates by combining SGEM and the block-diagonal complete-data FIM.

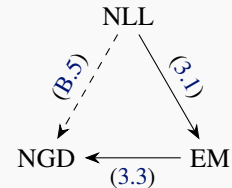


Figure 3. Key concepts and connections in §3.2.

### 3.3. Natural Gradient EM

Drawing upon previous theoretical analyses (§3.2), we show in this section how one can combine the sGEM objective and the complete-data FIM  $\hat{F}(\phi^{(x)})$  of Gaussian mixtures (17) to derive tractable natural gradient EM updates for MDNs. Specifically, we leverage the block-diagonal structure of  $\hat{F}(\phi^{(x)})$ , which essentially factorizes an NGD update on Gaussian mixture parameters  $\phi^{(x)}$  into  $K + 1$  independent NGD updates on each categorical or Gaussian distribution.

To motivate the factorization perspective, we first rewrite the sGEM objective (16) into the following identical but factorized nGEM objective:

$$\begin{aligned} \mathcal{L}_{\text{nGEM}}(\boldsymbol{\theta}) = & H\left(\left[\rho^{(x)}\right], \boldsymbol{\pi}^{(x)}\right) \\ & - \sum_{k=1}^K \left[\rho_k^{(x)}\right] \log \mathcal{N}(\mathbf{y}; \boldsymbol{\mu}_k^{(x)}, \boldsymbol{\Sigma}_k^{(x)}), \end{aligned} \quad (18)$$

where the first term is the cross-entropy between  $\rho^{(x)}$  and  $\boldsymbol{\pi}^{(x)}$ , and the other  $K$  terms are the negative log-likelihoods of the Gaussian components weighted by  $\rho_k^{(x)}$ .

The nGEM objective builds on sGEM by preconditioning the gradients with the complete-data FIM. We denote the gradient of the nGEM objective w.r.t.  $\phi^{(x)}$  as

$$\nabla_{\phi^{(x)}} = [\nabla_1 \quad \cdots \quad \nabla_K \quad \nabla_{\boldsymbol{\pi}}]^\top, \quad (19)$$

where  $\nabla_k$  for  $k \in \{1, \dots, K\}$  is the gradient of the  $k$ -th Gaussian, and  $\nabla_{\boldsymbol{\pi}}$  is the gradient of categorical distribution. Therefore, the complete-data natural gradient w.r.t.  $\phi^{(x)}$  is

$$\begin{aligned} \hat{\nabla}_{\phi^{(x)}} &= \hat{F}(\phi^{(x)})^{-1} \nabla_{\phi^{(x)}} \\ &= \left[ \frac{F_1^{-1}}{\boldsymbol{\pi}_1} \nabla_1 \quad \cdots \quad \frac{F_K^{-1}}{\boldsymbol{\pi}_K} \nabla_K \quad F_{\boldsymbol{\pi}}^{-1} \nabla_{\boldsymbol{\pi}} \right]^\top, \end{aligned} \quad (20)$$

due to the block-diagonal structure of  $\hat{F}(\phi^{(x)})$ .

We thus show that the complete-data natural gradient  $\hat{\nabla}_{\phi^{(x)}}$ , which is core to the natural gradient EM updates (17), can be easily computed by preconditioning the regular gradient  $\nabla_{\phi^{(x)}}$  with the inverse of FIMs of individual distributions. For the exponential family distributions (including Gaussian and categorical), Khan & Rue (2023) demonstrate that their natural gradients are often *easy* to compute.

For **Gaussian** distributions, we adopt the common assumption of diagonal covariances in deep learning (Kingma & Welling, 2013). We show in §B.6 that for Gaussians parametrized by the mean  $\boldsymbol{\mu}$  and (diagonal) standard deviation  $\boldsymbol{\sigma}$ , we have the following analytical *diagonal* FIM

$$F([\boldsymbol{\mu} \quad \boldsymbol{\sigma}]) = \begin{bmatrix} \frac{1}{\boldsymbol{\sigma}^2} & 0 \\ 0 & \frac{2}{\boldsymbol{\sigma}^2} \end{bmatrix}. \quad (21)$$

For **categorical** distributions parametrized by the logits  $\boldsymbol{\psi}$  such that probabilities  $\boldsymbol{\pi} = \text{softmax}(\boldsymbol{\psi})$ , we also derive in §B.7 that the analytical FIM is

$$F(\boldsymbol{\psi}) = \text{diag}(\boldsymbol{\pi}) - \boldsymbol{\pi}\boldsymbol{\pi}^\top, \quad (22)$$

which is, however, rank-deficient ( $\text{rank}(F(\boldsymbol{\psi})) = K - 1$ ) and hence not directly invertible. We replace  $F(\boldsymbol{\psi})^{-1}$  with the Moore-Penrose pseudo-inverse in practice.

We have so far derived analytical FIMs for categorical and Gaussian distributions (with specific parametrization). We now present the complete natural gradient EM algorithm for optimizing mixture density networks as follows<sup>6</sup>:

---

**Algorithm 1** Natural Gradient Expectation Maximization

**Initialize:** Training set  $\mathcal{D} = \{\mathbf{x}_n, \mathbf{y}_n\}_{n=1}^N$ , mixture density network  $f(\mathbf{x}; \boldsymbol{\theta}_0)$ , learning rate  $\beta$ , maximum iterations  $T$ .

- 1: **for** each iteration  $t \in \{1, \dots, T\}$  **do**
- 2:    Sample  $(\mathbf{x}, \mathbf{y}) \sim \mathcal{D}$  from the training set
- 3:    Compute  $\phi^{(x)} = \{\boldsymbol{\pi}_k^{(x)}, \boldsymbol{\mu}_k^{(x)}, \boldsymbol{\sigma}_k^{(x)}\}_{k=1}^K = f(\mathbf{x}; \boldsymbol{\theta}_t)$
- 4:    **(E-step)** Compute the responsibilities  $\rho^{(x)}$  (15)

$$\rho_k^{(x)} = \frac{\boldsymbol{\pi}_k^{(x)} \mathcal{N}(\mathbf{y}; \boldsymbol{\mu}_k^{(x)}, \boldsymbol{\sigma}_k^{(x)})}{\sum_{j=1}^K \boldsymbol{\pi}_j^{(x)} \mathcal{N}(\mathbf{y}; \boldsymbol{\mu}_j^{(x)}, \boldsymbol{\sigma}_j^{(x)})}$$

**(M-step)**

- 5:    Compute regular gradients  $\nabla_{\phi^{(x)}}$  (19) of  $\mathcal{L}_{\text{nGEM}}$  (18)
- 6:    Compute the FIMs  $F_1, \dots, F_K, F_{\boldsymbol{\pi}}$  of Gaussian (21) and categorical (22) distributions
- 7:    Compute complete-data natural gradients  $\hat{\nabla}_{\phi^{(x)}}$  (20)
- 8:    Update the mixture density network parameters  $\boldsymbol{\theta}$  via chain rule and backpropagation

$$\boldsymbol{\theta}_{t+1} \leftarrow \boldsymbol{\theta}_t - \beta \hat{\nabla}_{\phi^{(x)}} \nabla_{\boldsymbol{\theta}} \phi^{(x)}$$

- 9: **end for**

**Return:** optimized mixture density network  $f(\mathbf{x}; \boldsymbol{\theta}_T)$

---

Algorithm 1 can be easily extended to the mini-batch case by summing or averaging  $\hat{\nabla}_{\phi^{(x)}}$  across samples  $\mathbf{x}$ . We also provide example implementation of the algorithm in JAX (Bradbury et al., 2018) in Section C, which amounts to only few lines of custom auto-differentiation hooks.

### 3.4. Interpretation

In this section, we provide further justifications to intuit how nGEM exploits the information geometry to improve learning mixture density networks.

Recall that NGD penalizes the KL divergence between the distributions induced by a parameter update. As an example,

<sup>6</sup>Note that we use a learning rate  $\beta < 1$  in practice for stability.

consider two univariate Gaussians  $p$  and  $q$  with the same variance  $\sigma^2$ . Their KL divergence between is given by

$$\mathbb{D}_{\text{KL}}(p\|q) = (\mu_1 - \mu_2)^2 / (2\sigma^2), \quad (23)$$

which implies that Gaussians with lower variances are more sensitive to parameter updates<sup>7</sup>, and vice versa. Our nGEM partially works as an automatic learning rate scheduler that scales the gradients of Gaussian components proportionally to their variances  $\sigma^2$  (21), allowing the model to quickly jump through high-variance regions while taking conservative steps in low-variance regions, leading to faster and more stable convergence.

Furthermore, Chen et al. (2024) show that *all* local minima of the Gaussian mixture NLL is a combination of (a) one component covering multiple ground-truth Gaussians and (b) multiples components converging to one ground-truth Gaussian. For the former case, the covering Gaussian must have high variance  $\sigma^2$  to cover multiple modes, and nGEM allows escaping such mode collapsing local minima by again amplifying the gradients proportionally to  $\sigma^2$ .

## 4. Experiments

We now present experiments<sup>8</sup> designed to answer the following key research questions:

- (§4.1) Does nGEM generally yield faster convergence?
- (§4.2) Does nGEM help mitigate or prevent mode collapse?
- (§4.3) How does nGEM work with high-dimensional data?
- (§4.4) How does nGEM perform against baselines on real-world predictive tasks? How much computational overhead does nGEM incur?

### 4.1. Measuring Convergence

We start by measuring the convergence rates of nGEM on two synthetic examples, of which we have access to the ground-truth distributions for comparison and evaluation. The first synthetic example is the **Two-Gaussians** dataset, which contains  $2n$  training data points equally sampled from two distinct and well-separated Gaussians in  $\mathbb{R}^2$ , as illustrated in Figures 2a and 2b.

Two-Gaussians is a simple *illustrative* task that does not require a neural network to model conditional distributions. Instead we directly learn the Gaussian mixture parameters using either nGEM or NLL. Figure 4 illustrates how nGEM performs against the standard NLL on this task with different learning rates  $\beta$  by measuring their negative log-likelihoods. We find that nGEM consistently outperforms NLL in terms of convergence rates: (a) nGEM can converge with only around 500 iterations while NLL takes over 5000 iterations

<sup>7</sup>A small change  $\mu_1 - \mu_2$  results in a large KL divergence.

<sup>8</sup>Hyperparameters are provided in §D.1 for reference.

( $\beta = 10^{-2}$ ), and (b) nGEM can reliably converge to the optimal solution whereas NLL catastrophically fails due to mode collapse ( $\beta = 10^{-1}$ ).

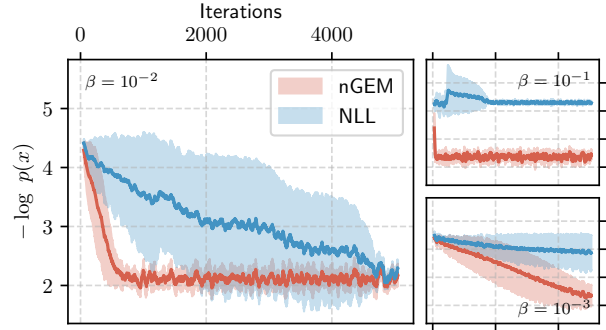


Figure 4. Negative log-likelihood ( $\downarrow$ ) of the learned GMM on the Two-Gaussians example, with different learning rates  $\beta$ . Results averaged ( $\pm$  std) across 5 random seeds.

Figure 5 visualizes the trajectories of the learned Gaussian mixture component means during one training. We observe that nGEM (Figure 5a) moves along a straight path towards the targets (\*), presumably owing to nGEM’s awareness of the information geometry. Furthermore, nGEM takes larger jumps in early iterations and switches to smaller steps near convergence, aligning with our discussion in §3.4. On the other hand, NLL (Figure 5b) moves along a curved path with fixed step sizes, resulting in slower convergence.

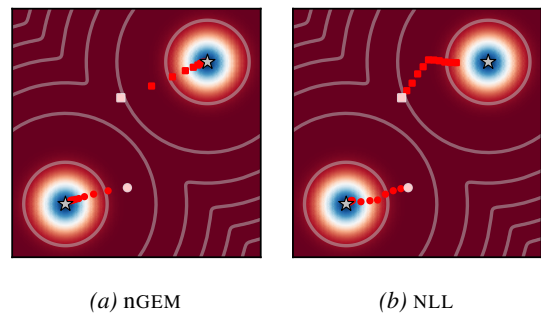


Figure 5. Trajectories of the GMM ( $K = 2$ ) component means on the Two-Gaussians example during training. Stars (\*) represent the ground-truth Gaussian means, white squares/circles represent the initial component means, and their red counterparts represent the trajectory of component means logged periodically during training.

The second synthetic example is the **Two-Sinusoids** dataset, which requires modeling a conditional density  $p(y|x)$  such that  $x \sim \text{Uniform}(0, 4\pi)$  and  $y$  is equally probably one of  $\pi \sin(x) + \xi$  or  $\pi \sin(x + \pi) + \xi$ , with  $\xi$  being an additive Gaussian noise sampled from  $\mathcal{N}(0, 0.1)$ . We adopt a standard multi-layer perceptron (MLP) backbone for MDN, and optimize the network parameters using either nGEM or NLL.

Figure 6 illustrates how nGEM performs against standard NLL on this task with different learning rates  $\beta$ . We find

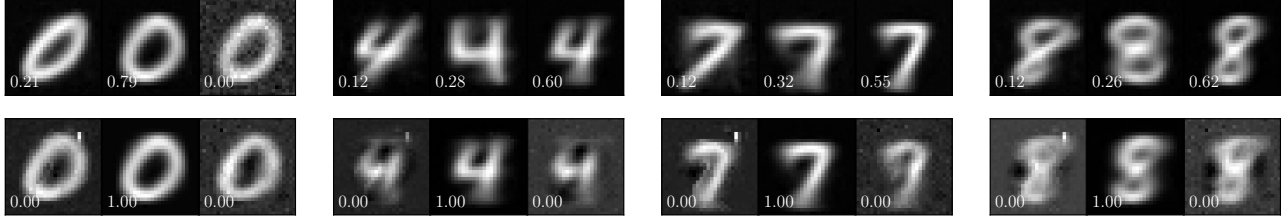


Figure 8. **Top row** (nGEM) v.s. **Bottom row** (NLL). Visualizing the predicted Gaussian mixture ( $K = 3$ ) component means  $\mu_k$  given class labels  $\{0, 4, 7, 8\}$  on the inverse MNIST example. Numbers to the bottom left corner of each image denote the corresponding mixture component weight  $\pi_k$ . We refer the readers to §D.2 for full visualization results due to space constraint.

that nGEM still generally outperforms NLL, exhibiting faster and more stable convergence across learning rates.

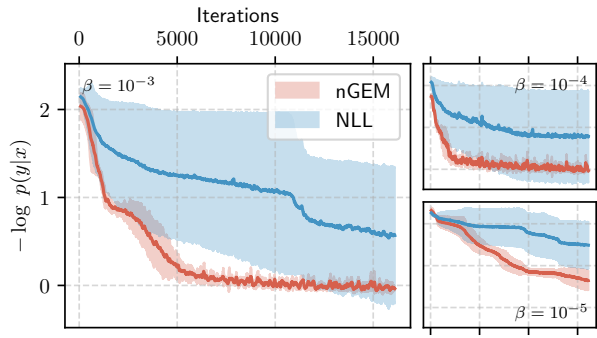


Figure 6. Negative log-likelihood ( $\downarrow$ ) of the learned MDN on the Two-Sinusoids example, with different learning rates  $\beta$ . Results averaged ( $\pm$  std) across 5 random seeds.

Figure 7 demonstrates that nGEM can learn two separate conditional Gaussians to approximate the sine waves, while NLL suffers from mode collapse and only uses one high-variance Gaussian (red) to cover both modes.

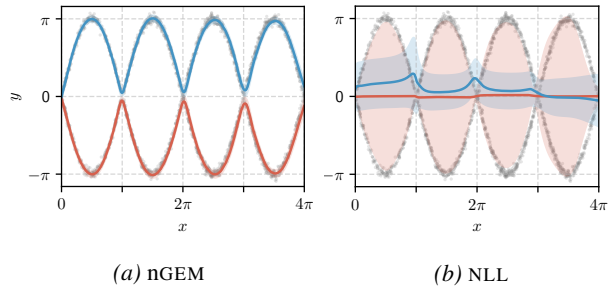


Figure 7. Visualization of the learned conditional mixture density ( $K = 2$ ) on the Two-Sinusoids example for one training. Gray dots in the background represent the training samples, and the red and blue bands represent the means ( $\pm$  std) of the two Gaussian components conditioned on the input  $x$ .

#### 4.2. Measuring Mode Collapse

For evaluating mode collapse, we reuse the two synthetic examples, of which we know the optimal mixture weight is

given by  $\pi^* = [0.5, 0.5]$ . We assess the severity of mode collapse by comparing the entropy  $H(\pi)$  of the learned mixture weights against the optimal entropy  $H(\pi^*) \approx 0.693$ .

Table 1 summarizes the learned mixture weight's entropy  $H(\pi)$  on Two-Gaussians with different learning rates  $\beta$ . Note that nGEM consistently learns near-optimal mixture weights, while NLL exhibits mode collapse for  $\beta = 10^{-1}$ .

Table 1. Entropy ( $\uparrow$ ) of the learned mixture weight  $\pi$  on the Two-Gaussians example, with different learning rates  $\beta$ . Results averaged ( $\pm$  std) across 5 random seeds.

Method	$\beta = 10^{-1}$	$\beta = 10^{-2}$	$\beta = 10^{-3}$
nGEM	<b><math>0.660 \pm 0.03</math></b>	<b><math>0.691 \pm 0.00</math></b>	<b><math>0.692 \pm 0.00</math></b>
NLL	$0.010 \pm 0.00$	$0.687 \pm 0.01$	$0.669 \pm 0.02$

Table 2 summarizes the learned mixture weight's entropy  $H(\pi)$  on Two-Sinusoids with different learning rates  $\beta$ . For this task, nGEM can again consistently learn near-optimal mixture weights, whereas NLL is unstable (high std) and suffers from mode collapse across learning rates.

Table 2. Entropy ( $\uparrow$ ) of the learned mixture weight  $\pi$  on the Two-Sinusoids example, with different learning rates  $\beta$ . Results averaged ( $\pm$  std) across 5 random seeds.

Method	$\beta = 10^{-3}$	$\beta = 10^{-4}$	$\beta = 10^{-5}$
nGEM	<b><math>0.693 \pm 0.00</math></b>	<b><math>0.693 \pm 0.00</math></b>	<b><math>0.693 \pm 0.00</math></b>
NLL	$0.416 \pm 0.38$	$0.555 \pm 0.31$	$0.413 \pm 0.38$

#### 4.3. Modeling High-Dimensional Data

We proceed to investigate how well nGEM scales to high-dimensional data. We consider the **inverse MNIST** problem, where one aims to predict the handwritten digit image  $x \in \mathbb{R}^{28 \times 28}$  given its class label  $y \in \{0, \dots, 9\}$ .

Figure 8 inspects the predicted Gaussian mixture ( $K = 3$ ) component means given labels. We observe that nGEM (**top row**) can use different components to capture subtle style variations and predict sharp images. On the other hand, NLL (**bottom row**) suffers from mode collapse (some  $\pi_k = 1$ )

Table 5. Negative log-likelihoods ( $\downarrow$ ) and rooted mean squared errors (RMSE,  $\downarrow$ ) of 10 baselines on test datasets for 3 regression tasks. Results are averaged ( $\pm$  std) across 5 random seeds. Note that (a) negative log-likelihoods are not available for MSE, (b) RMSE for Gaussians ( $\beta$ -NLL) is computed between the mean and the target, i.e.  $\text{RMSE}(\boldsymbol{\mu}, \mathbf{y})$ , and (c) RMSE for Gaussian mixtures (nGEM/NLL) is computed as the minimum RMSE between each Gaussian component mean and the target, i.e.  $\min_k \text{RMSE}(\boldsymbol{\mu}_k, \mathbf{y})$ .

Method	Negative Log-Likelihood ( $\downarrow$ )			RMSE ( $\downarrow$ ) $\times 10^1$		
	kin8nm	energy	housing	kin8nm	energy	housing
Adam + nGEM	-1.73 $\pm$ 0.04	-3.29 $\pm$ 0.13	-0.39 $\pm$ 0.06	0.17 $\pm$ 0.01	0.49 $\pm$ 0.04	0.81 $\pm$ 0.07
+ NLL	-1.67 $\pm$ 0.06	-3.09 $\pm$ 0.24	-0.67 $\pm$ 0.12	0.33 $\pm$ 0.03	0.95 $\pm$ 0.12	1.02 $\pm$ 0.05
KFAC + nGEM	-0.69 $\pm$ 0.02	-0.43 $\pm$ 0.01	1.15 $\pm$ 0.06	0.65 $\pm$ 0.03	1.51 $\pm$ 0.03	4.43 $\pm$ 0.60
+ NLL	-1.64 $\pm$ 0.08	-0.96 $\pm$ 0.08	1.24 $\pm$ 0.05	0.31 $\pm$ 0.02	2.11 $\pm$ 0.35	5.11 $\pm$ 0.80
Muon + nGEM	-1.84 $\pm$ 0.05	-3.19 $\pm$ 0.08	-0.19 $\pm$ 0.02	0.15 $\pm$ 0.00	0.53 $\pm$ 0.01	1.03 $\pm$ 0.11
+ NLL	-1.80 $\pm$ 0.06	-2.68 $\pm$ 0.17	-0.24 $\pm$ 0.01	0.25 $\pm$ 0.00	1.32 $\pm$ 0.18	1.51 $\pm$ 0.11
Soap + nGEM	<b>-1.96 <math>\pm</math> 0.05</b>	<b>-4.18 <math>\pm</math> 0.10</b>	-0.48 $\pm$ 0.14	<b>0.11 <math>\pm</math> 0.01</b>	<b>0.30 <math>\pm</math> 0.01</b>	<b>0.77 <math>\pm</math> 0.09</b>
+ NLL	-1.93 $\pm$ 0.06	-3.99 $\pm$ 0.18	<b>-0.79 <math>\pm</math> 0.11</b>	0.21 $\pm$ 0.01	0.72 $\pm$ 0.05	1.00 $\pm$ 0.09
Adam + $\beta$ -NLL	-1.60 $\pm$ 0.02	-2.55 $\pm$ 0.16	-0.22 $\pm$ 0.05	0.40 $\pm$ 0.01	0.97 $\pm$ 0.04	1.65 $\pm$ 0.10
+ MSE	—	—	—	0.39 $\pm$ 0.01	0.95 $\pm$ 0.02	1.42 $\pm$ 0.04

and can only predict blurry, visually similar images.

Table 3. Negative log-likelihood ( $\downarrow$ ) and entropy ( $\uparrow$ ) of the learned MDN ( $K = 3$ ) for inverse MNIST. We use the same hyperparameters and average metrics ( $\pm$  std) across 5 random seeds.

Method	$-\log p(\mathbf{x} \mathbf{y})$ ( $\downarrow$ )	$H(\boldsymbol{\pi})$ ( $\uparrow$ )
nGEM	<b>-1529.7 <math>\pm</math> 101</b>	<b>0.454 <math>\pm</math> 0.15</b>
NLL	-1392.8 $\pm$ 178	0.207 $\pm$ 0.22

Table 3 summarizes the learned mixture density network’s negative log-likelihood and entropy on the inverse MNIST problem. We find that overall nGEM outperforms NLL with lower negative log-likelihood and higher entropy.

We also examine the over-parametrized setting, where we set the mixture density networks to have  $K = 10$  components. Table 4 shows that nGEM can perform reliably even in such challenging settings.

Table 4. Negative log-likelihood ( $\downarrow$ ) and entropy ( $\uparrow$ ) of the learned MDN ( $K = 10$ ) for inverse MNIST. We use the same hyperparameters and average metrics ( $\pm$  std) across 5 random seeds.

Method	$-\log p(\mathbf{x} \mathbf{y})$ ( $\downarrow$ )	$H(\boldsymbol{\pi})$ ( $\uparrow$ )
nGEM	<b>-1601.4 <math>\pm</math> 146</b>	<b>0.688 <math>\pm</math> 0.00</b>
NLL	-1470.0 $\pm$ 148	0.456 $\pm$ 0.32

#### 4.4. Ablation Studies

We conduct additional baseline experiments on three standard real-world predictive modeling tasks from the UCI datasets (Hernandez-Lobato & Adams, 2015), involving robot kinematics (kin8nm), energy efficiency (energy), and Boston housing price regression (housing).

For baselines, we consider mixture density networks optimized with nGEM/NLL and different optimizers, including

Adam (Kingma & Ba, 2017) and other curvature-aware preconditioning gradient optimizers: KFAC (Martens & Grosse, 2015), Muon (Liu et al., 2025) and Soap (Vyas et al., 2025). We also consider  $\beta$ -NLL (Seitzer et al., 2022), which uses conditional Gaussian distributions for predictive modeling, and the canonical mean squared error (MSE) for regression.

Table 5 reports the the performance of each baseline on all datasets. We summarize our findings as follows:

- Mixture density networks with nGEM/NLL in general outperform  $\beta$ -NLL and MSE.
- When using the same optimizer, nGEM outperforms NLL in RMSE on all tasks, and also in log-likelihoods except housing (which is due to nGEM overfitting on the train set).
- The Soap optimizer combined with nGEM in general performs best, in terms of log-likelihoods and RMSE.

In particular, Table 5 highlight that nGEM is not competing with, but complementary to other preconditioning gradient optimizers. Our proposed nGEM operates in the Gaussian mixture distribution space, orthogonal to the neural network parameter space where other optimizers operate in. In fact, we find that integrating both methods yields additive performance gains that surpass either one in isolation.

Table 6 reports the wall-clock time ( $\downarrow$ ) of nGEM and NLL running for  $10^4$  gradient updates with Adam optimizer on 3 regression tasks. Results are averaged ( $\pm$  std) across 5 runs.

Method	kin8nm	energy	housing
nGEM	9.38 $\pm$ 0.08s	9.40 $\pm$ 0.05s	9.37 $\pm$ 0.05s
NLL	9.33 $\pm$ 0.06s	9.31 $\pm$ 0.08s	9.31 $\pm$ 0.11s

## 5. Related Work

**$\beta$ -NLL** (Seitzer et al., 2022) is a method for predictive uncertainty estimation by weighting the Gaussian NLL with a  $\beta$ -exponentiated variance  $\sigma^{2\beta}$ . Our proposed method nGEM decomposes into  $\beta$ -NLL when  $K = 1$  and  $\beta = 1$ , in which case preconditioning gradients with the inverse Gaussian FIM (21) is equivalent (up to constants) to weighting the Gaussian NLL objective with  $\sigma^2$ .

**Applications** Mixture density networks have grown popular for many downstream deep learning applications, for instance speech synthesis (Capes et al., 2017), model-based reinforcement learning (Ha & Schmidhuber, 2018), sketch generation (Ha & Eck, 2018), drone trajectory prediction (Makansi et al., 2019), and human pose estimation (Li & Lee, 2019). However, systematic investigations into learning objective pathologies of MDNs has remained scarce.

**Variational Inference** Though orthogonal to our work, Gaussian mixtures have also been used as surrogate posteriors in variational Bayesian inference (Lin et al., 2019; Morningstar et al., 2021; Arenz et al., 2023). For variational inference, one typically seeks to approximate an intractable posterior  $p(\mathbf{z}|\mathbf{x})$  by minimizing the KL divergence between a flexible surrogate  $q(\mathbf{z}|\mathbf{x})$  and the posterior. However, a key distinction is that in variational inference, one typically does not have access to samples from the target distribution for learning (in contrast to our work).

## 6. Conclusion

In this work, we introduce natural gradient expectation maximization (nGEM) for mixture density network optimization. We identify theoretical connections between EM and NGD to derive tractable natural gradient EM updates for MDN. Our proposed method nGEM can stabilize and accelerate learning mixture density networks, incurs negligible computational overheads, while remaining easy to implement in practice (see Section C).

Our empirical evaluations across a range of tasks – from synthetic examples to high-dimensional inverse problems – suggest that nGEM is both effective and robust. We expect nGEM to become a *drop-in* alternative to the standard NLL objective for learning deep mixture density networks.

**Limitations and Future Work** One of the fundamental assumption we rely on is the diagonal Gaussian covariance matrix, which is, although common in deep learning, still restrictive. An interesting future research direction would be deriving tractable natural gradient EM updates for Gaussian components with low-rank covariance approximations. Another future direction would be extending nGEM to non-Gaussian mixture models within the exponential family.

## Impact Statement

This paper presents work whose goal is to advance the field of Machine Learning. There are many potential societal consequences of our work, none which we feel must be specifically highlighted here.

## References

Amari, S.-i. Natural gradient works efficiently in learning. *Neural Computation*, 10(2):251–276, 1998. doi: 10.1162/089976698300017746.

Arenz, O., Dahlinger, P., Ye, Z., Volpp, M., and Neumann, G. A unified perspective on natural gradient variational inference with Gaussian mixture models. *Transactions on Machine Learning Research*, 2023. ISSN 2835-8856. URL <https://openreview.net/forum?id=tLBjsX4tjs>.

Bishop, C. *Pattern Recognition and Machine Learning*. Springer, January 2006.

Bishop, C. M. Mixture density networks. 1994.

Bradbury, J., Frostig, R., Hawkins, P., Johnson, M. J., Leary, C., Maclaurin, D., Necula, G., Paszke, A., VanderPlas, J., Wanderman-Milne, S., and Zhang, Q. JAX: composable transformations of Python+NumPy programs, 2018. URL <http://github.com/jax-ml/jax>.

Capes, T., Coles, P., Conkie, A., Golipour, L., Hadjitarkhani, A., Hu, Q., Huddleston, N., Hunt, M., Li, J., Neeracher, M., Prahallad, K., Raitio, T., Rasipuram, R., Townsend, G., Williamson, B., Winarsky, D., Wu, Z., and Zhang, H. Siri on-device deep learning-guided unit selection text-to-speech system. In *Interspeech 2017*, pp. 4011–4015, 2017. doi: 10.21437/Interspeech.2017-1798.

Chen, Y., Song, D., Xi, X., and Zhang, Y. Local minima structures in Gaussian mixture models. *IEEE Transactions on Information Theory*, 70(6):4218–4257, 2024. doi: 10.1109/TIT.2024.3374716.

Dempster, A. P., Laird, N. M., and Rubin, D. B. Maximum likelihood from incomplete data via the EM algorithm. *Journal of the royal statistical society: series B (methodological)*, 39(1):1–22, 1977.

Ha, D. and Eck, D. A neural representation of sketch drawings. In *International Conference on Learning Representations*, 2018. URL <https://openreview.net/forum?id=Hy6GHpkCW>.

Ha, D. and Schmidhuber, J. Recurrent world models facilitate policy evolution. In Bengio, S., Wallach, H., Larochelle, H., Grauman, K., Cesa-Bianchi, N., and Garnett, R. (eds.), *Advances in Neural Information Processing Systems*, volume 31. Curran Associates, Inc., 2018.

Hendrycks, D. and Gimpel, K. Gaussian error linear units (GELUs), 2023. URL <https://arxiv.org/abs/1606.08415>.

Hernandez-Lobato, J. M. and Adams, R. Probabilistic back-propagation for scalable learning of Bayesian neural networks. In Bach, F. and Blei, D. (eds.), *Proceedings of the 32nd International Conference on Machine Learning*, volume 37 of *Proceedings of Machine Learning Research*, pp. 1861–1869, Lille, France, 07–09 Jul 2015. PMLR. URL <https://proceedings.mlr.press/v37/hernandez-lobatoc15.html>.

Khan, M. E. and Rue, H. The Bayesian learning rule. *Journal of Machine Learning Research*, 24(281):1–46, 2023. URL <http://jmlr.org/papers/v24/22-0291.html>.

Kingma, D. P. and Ba, J. Adam: A method for stochastic optimization, 2017. URL <https://arxiv.org/abs/1412.6980>.

Kingma, D. P. and Welling, M. Auto-encoding variational Bayes. In *International Conference on Learning Representations*, 2013. URL <https://openreview.net/forum?id=33X9fd2-9FyZd>.

Li, C. and Lee, G. H. Generating multiple hypotheses for 3D human pose estimation with mixture density network. In *Proceedings of the IEEE/CVF Conference on Computer Vision and Pattern Recognition (CVPR)*, pp. 9887–9895, June 2019.

Lin, W., Khan, M. E., and Schmidt, M. Fast and simple natural-gradient variational inference with mixture of exponential-family approximations. In Chaudhuri, K. and Salakhutdinov, R. (eds.), *Proceedings of the 36th International Conference on Machine Learning*, volume 97 of *Proceedings of Machine Learning Research*, pp. 3992–4002. PMLR, 09–15 Jun 2019. URL <https://proceedings.mlr.press/v97/lin19b.html>.

Liu, J., Su, J., Yao, X., Jiang, Z., Lai, G., Du, Y., Qin, Y., Xu, W., Lu, E., Yan, J., Chen, Y., Zheng, H., Liu, Y., Liu, S., Yin, B., He, W., Zhu, H., Wang, Y., Wang, J., Dong, M., Zhang, Z., Kang, Y., Zhang, H., Xu, X., Zhang, Y., Wu, Y., Zhou, X., and Yang, Z. Muon is scalable for llm training, 2025. URL <https://arxiv.org/abs/2502.16982>.

Makansi, O., Ilg, E., Cicek, O., and Brox, T. Overcoming limitations of mixture density networks: A sampling and fitting framework for multimodal future prediction. In *Proceedings of the IEEE/CVF Conference on Computer Vision and Pattern Recognition*, pp. 7144–7153, June 2019.

Martens, J. New insights and perspectives on the natural gradient method. *Journal of Machine Learning Research*, 21(146):1–76, 2020. URL <http://jmlr.org/papers/v21/17-678.html>.

Martens, J. and Grosse, R. Optimizing neural networks with kronecker-factored approximate curvature. In Bach, F. and Blei, D. (eds.), *Proceedings of the 32nd International Conference on Machine Learning*, volume 37 of *Proceedings of Machine Learning Research*, pp. 2408–2417, Lille, France, 07–09 Jul 2015. PMLR. URL <https://proceedings.mlr.press/v37/martens15.html>.

Morningstar, W., Vikram, S., Ham, C., Gallagher, A., and Dillon, J. Automatic differentiation variational inference with mixtures. In Banerjee, A. and Fukumizu, K. (eds.), *Proceedings of The 24th International Conference on Artificial Intelligence and Statistics*, volume 130 of *Proceedings of Machine Learning Research*, pp. 3250–3258. PMLR, 13–15 Apr 2021. URL <https://proceedings.mlr.press/v130/morningstar21b.html>.

Neal, R. M. and Hinton, G. E. A view of the EM algorithm that justifies incremental, sparse, and other variants. In *Learning in graphical models*, pp. 355–368. Springer, 1998.

Salakhutdinov, R., Roweis, S. T., and Ghahramani, Z. Optimization with EM and expectation-conjugate-gradient. In *Proceedings of the 20th International Conference on Machine Learning*, pp. 672–679, 2003.

Sato, M.-A. Online model selection based on the variational Bayes. *Neural computation*, 13(7):1649–1681, 2001.

Seitzer, M., Tavakoli, A., Antic, D., and Martius, G. On the pitfalls of heteroscedastic uncertainty estimation with probabilistic neural networks. In *International Conference on Learning Representations*, 2022. URL <https://openreview.net/forum?id=aPOpXlnV1T>.

Vyas, N., Morwani, D., Zhao, R., Shapira, I., Brandfonbrener, D., Janson, L., and Kakade, S. M. SOAP: Improving and stabilizing Shampoo using Adam for language modeling. In *The Thirteenth International Conference on Learning Representations*, 2025. URL <https://openreview.net/forum?id=IDxZhXrpNf>.

Xu, W., Fazel, M., and Du, S. S. Toward global convergence of gradient EM for over-paramterized Gaussian mixture models. In Globerson, A., Mackey, L., Belgrave, D., Fan, A., Paquet, U., Tomczak, J., and Zhang, C. (eds.), *Advances in Neural Information Processing Systems*, volume 37, pp. 10770–10800. Curran Associates, Inc., 2024. doi: 10.5220/079017-0344.

## A. Natural Gradient Descent

In machine learning, the gradient descent algorithm for minimizing some objective function  $J(\boldsymbol{\theta}) : \mathbb{R}^n \rightarrow \mathbb{R}$  is

$$\boldsymbol{\theta}_{t+1} \leftarrow \boldsymbol{\theta}_t - \beta \nabla J(\boldsymbol{\theta}_t), \quad (24)$$

where  $\beta$  is commonly known as the *learning rate*.

One can show that the above gradient descent update can be derived from minimizing the first-order Taylor expansion of  $J(\boldsymbol{\theta})$  at  $\boldsymbol{\theta} = \boldsymbol{\theta}_t$  with an additional Euclidean distance penalty

$$\boldsymbol{\theta}_{t+1} = \arg \min_{\boldsymbol{\theta}} \underbrace{J(\boldsymbol{\theta}_t) + \nabla J(\boldsymbol{\theta}_t)^\top (\boldsymbol{\theta} - \boldsymbol{\theta}_t)}_{\text{Taylor expansion}} + (2\beta)^{-1} \underbrace{\|\boldsymbol{\theta} - \boldsymbol{\theta}_t\|_2^2}_{\text{Penalty}}. \quad (25)$$

Therefore, we say that gradient descent implicitly assumes that the model parameters  $\boldsymbol{\theta}$  lives in a *Euclidean space* by using a Euclidean distance penalty to constrain large updates. However, for probabilistic models  $p(\mathbf{x}|\boldsymbol{\theta})$ , the parameter space is generally not Euclidean. Instead, a more natural penalty term would be the Kullback-Leibler (KL) divergence between the induced distributions, resulting in the following optimization objective

$$\boldsymbol{\theta}_{t+1} = \arg \min_{\boldsymbol{\theta}} J(\boldsymbol{\theta}_t) + \nabla J(\boldsymbol{\theta}_t)^\top (\boldsymbol{\theta} - \boldsymbol{\theta}_t) + \beta^{-1} \underbrace{\mathbb{D}_{\text{KL}}(p(\mathbf{x}|\boldsymbol{\theta}_t) \| p(\mathbf{x}|\boldsymbol{\theta}))}_{\text{Penalty}}. \quad (26)$$

Since  $\mathbb{D}_{\text{KL}}(p\|q)$  does not have an analytical form generally, we instead consider its second-order Taylor expansion at  $\boldsymbol{\theta} = \boldsymbol{\theta}_t$

$$\begin{aligned} \mathbb{D}_{\text{KL}}(p(\mathbf{x}|\boldsymbol{\theta}_t) \| p(\mathbf{x}|\boldsymbol{\theta})) &\approx \mathbb{D}_{\text{KL}}(p(\mathbf{x}|\boldsymbol{\theta}_t) \| p(\mathbf{x}|\boldsymbol{\theta}_t)) \\ &\quad + (\nabla_{\boldsymbol{\theta}} \mathbb{D}_{\text{KL}}(p(\mathbf{x}|\boldsymbol{\theta}_t) \| p(\mathbf{x}|\boldsymbol{\theta}))|_{\boldsymbol{\theta}=\boldsymbol{\theta}_t})^\top (\boldsymbol{\theta} - \boldsymbol{\theta}_t) \\ &\quad + \frac{1}{2} (\boldsymbol{\theta} - \boldsymbol{\theta}_t)^\top (\nabla_{\boldsymbol{\theta}}^2 \mathbb{D}_{\text{KL}}(p(\mathbf{x}|\boldsymbol{\theta}_t) \| p(\mathbf{x}|\boldsymbol{\theta}))|_{\boldsymbol{\theta}=\boldsymbol{\theta}_t}) (\boldsymbol{\theta} - \boldsymbol{\theta}_t), \end{aligned} \quad (27)$$

where

1. The first term  $\mathbb{D}_{\text{KL}}(p(\mathbf{x}|\boldsymbol{\theta}_t) \| p(\mathbf{x}|\boldsymbol{\theta}_t))$  is trivially *zero*.
2. The second term is also *zero* because the expectation of the score function  $\nabla \log p(\mathbf{x})$  is zero.

$$\nabla_{\boldsymbol{\theta}} \mathbb{D}_{\text{KL}}(p(\mathbf{x}|\boldsymbol{\theta}_t) \| p(\mathbf{x}|\boldsymbol{\theta}))|_{\boldsymbol{\theta}=\boldsymbol{\theta}_t} = -\mathbb{E}_{p(\mathbf{x}|\boldsymbol{\theta}_t)} \left[ \underbrace{\nabla_{\boldsymbol{\theta}} \log p(\mathbf{x}|\boldsymbol{\theta}_t)}_{\text{Score}} \right] = 0. \quad (28)$$

3. The third term is  $\frac{1}{2} (\boldsymbol{\theta} - \boldsymbol{\theta}_t)^\top F(\boldsymbol{\theta}_t) (\boldsymbol{\theta} - \boldsymbol{\theta}_t)$ , where  $F(\boldsymbol{\theta}_t)$  is the Fisher information matrix (6) at  $\boldsymbol{\theta} = \boldsymbol{\theta}_t$ .

$$\nabla_{\boldsymbol{\theta}}^2 \mathbb{D}_{\text{KL}}(p(\mathbf{x}|\boldsymbol{\theta}_t) \| p(\mathbf{x}|\boldsymbol{\theta}))|_{\boldsymbol{\theta}=\boldsymbol{\theta}_t} = -\mathbb{E}_{p(\mathbf{x}|\boldsymbol{\theta}_t)} [\nabla_{\boldsymbol{\theta}}^2 \log p(\mathbf{x}|\boldsymbol{\theta}_t)] = F(\boldsymbol{\theta}_t). \quad (29)$$

Therefore, we have  $\mathbb{D}_{\text{KL}}(p(\mathbf{x}|\boldsymbol{\theta}_t) \| p(\mathbf{x}|\boldsymbol{\theta})) \approx \frac{1}{2} (\boldsymbol{\theta} - \boldsymbol{\theta}_t)^\top F(\boldsymbol{\theta}_t) (\boldsymbol{\theta} - \boldsymbol{\theta}_t)$ . Plugging back the approximation and solving the new optimization objective

$$\boldsymbol{\theta}_{t+1} = \arg \min_{\boldsymbol{\theta}} J(\boldsymbol{\theta}_t) + \nabla J(\boldsymbol{\theta}_t)^\top (\boldsymbol{\theta} - \boldsymbol{\theta}_t) + (2\beta)^{-1} \underbrace{(\boldsymbol{\theta} - \boldsymbol{\theta}_t)^\top F(\boldsymbol{\theta}_t) (\boldsymbol{\theta} - \boldsymbol{\theta}_t)}_{\text{Penalty}}. \quad (30)$$

lead to the following natural gradient descent (NGD) update

$$\boldsymbol{\theta}_{t+1} \leftarrow \boldsymbol{\theta}_t - \beta F^{-1}(\boldsymbol{\theta}_t) \nabla J(\boldsymbol{\theta}_t). \quad (31)$$

Natural gradient descent yields the steepest descent on a Riemannian manifold with the Fisher information metric, which subsumes the standard gradient descent on the Euclidean space as a special case when  $F(\boldsymbol{\theta}) = I$ .

## B. Proofs and Derivations

### B.1. Proof of Theorem 3.1

We assume a probabilistic model  $p(\mathbf{x}, \mathbf{z}|\boldsymbol{\theta})$  with observed variables  $\mathbf{x}$ , latent variables  $\mathbf{z}$ , and parameters  $\boldsymbol{\theta}$ .

We begin by rewriting the gradient of the observed-data log likelihood as follows:

$$\begin{aligned}
 \nabla_{\boldsymbol{\theta}} \log p(\mathbf{x}|\boldsymbol{\theta}) &= \frac{1}{p(\mathbf{x}|\boldsymbol{\theta})} \nabla_{\boldsymbol{\theta}} p(\mathbf{x}|\boldsymbol{\theta}) \\
 &= \frac{1}{p(\mathbf{x}|\boldsymbol{\theta})} \nabla_{\boldsymbol{\theta}} \int p(\mathbf{x}, \mathbf{z}|\boldsymbol{\theta}) d\mathbf{z} \\
 &= \frac{1}{p(\mathbf{x}|\boldsymbol{\theta})} \int \nabla_{\boldsymbol{\theta}} p(\mathbf{x}, \mathbf{z}|\boldsymbol{\theta}) d\mathbf{z} \\
 &= \frac{1}{p(\mathbf{x}|\boldsymbol{\theta})} \int p(\mathbf{x}, \mathbf{z}|\boldsymbol{\theta}) \nabla_{\boldsymbol{\theta}} \log p(\mathbf{x}, \mathbf{z}|\boldsymbol{\theta}) d\mathbf{z} \\
 &= \int p(\mathbf{z}|\mathbf{x}, \boldsymbol{\theta}) \nabla_{\boldsymbol{\theta}} \log p(\mathbf{x}, \mathbf{z}|\boldsymbol{\theta}) d\mathbf{z}.
 \end{aligned} \tag{32}$$

Note that by definition  $Q(\boldsymbol{\theta} \mid \boldsymbol{\theta}_t) = \int p(\mathbf{z}|\mathbf{x}, \boldsymbol{\theta}_t) \log p(\mathbf{x}, \mathbf{z}|\boldsymbol{\theta}) d\mathbf{z}$ . It is then clear that

$$\nabla_{\boldsymbol{\theta}} \log p(\mathbf{x}|\boldsymbol{\theta}) \Big|_{\boldsymbol{\theta}=\boldsymbol{\theta}_t} = \int p(\mathbf{z}|\mathbf{x}, \boldsymbol{\theta}_t) \nabla_{\boldsymbol{\theta}} \log p(\mathbf{x}, \mathbf{z}|\boldsymbol{\theta}_t) d\mathbf{z} = \nabla_{\boldsymbol{\theta}} Q(\boldsymbol{\theta} \mid \boldsymbol{\theta}_t) \Big|_{\boldsymbol{\theta}=\boldsymbol{\theta}_t}. \tag{33}$$

### B.2. Proof of Theorem 3.2

We view the mixture density network  $f(\mathbf{x}; \boldsymbol{\theta})$  as a latent variable model  $p(\mathbf{y}, \mathbf{z}|\mathbf{x}; \boldsymbol{\theta})$  with observed features  $\mathbf{x}$  and targets  $\mathbf{y}$ , latent variables  $\mathbf{z}$ , and network parameters  $\boldsymbol{\theta}$ .

Following Theorem 3.1, with a trivial substitution of  $p(\mathbf{x}, \mathbf{z}|\boldsymbol{\theta})$  with  $p(\mathbf{y}, \mathbf{z}|\mathbf{x}; \boldsymbol{\theta})$ , we can similarly derive that

$$\nabla_{\boldsymbol{\theta}} \log p(\mathbf{y}|\mathbf{x}; \boldsymbol{\theta}) = \int p(\mathbf{z}|\mathbf{x}, \mathbf{y}; \boldsymbol{\theta}) \nabla_{\boldsymbol{\theta}} \log p(\mathbf{y}, \mathbf{z}|\mathbf{x}; \boldsymbol{\theta}) d\mathbf{z}. \tag{34}$$

Recall that by definition we have

$$\mathcal{L}_{\text{NLL}}(\boldsymbol{\theta}) = -\log p(\mathbf{y}|\mathbf{x}; \boldsymbol{\theta}), \tag{35}$$

$$\mathcal{L}_{\text{SGEM}}(\boldsymbol{\theta}) = -\int p(\mathbf{z}|\mathbf{x}, \mathbf{y}; \boldsymbol{\theta}_t) \log p(\mathbf{y}, \mathbf{z}|\mathbf{x}; \boldsymbol{\theta}) d\mathbf{z}, \tag{36}$$

where  $\boldsymbol{\theta}_t$  is the parameter used for evaluating the responsibilities  $\rho^{(\mathbf{x})}$  (15).

Therefore, it is clear that

$$\nabla_{\boldsymbol{\theta}} \mathcal{L}_{\text{NLL}}(\boldsymbol{\theta}) \Big|_{\boldsymbol{\theta}=\boldsymbol{\theta}_t} = -\int p(\mathbf{z}|\mathbf{x}, \mathbf{y}; \boldsymbol{\theta}_t) \nabla_{\boldsymbol{\theta}} \log p(\mathbf{y}, \mathbf{z}|\mathbf{x}; \boldsymbol{\theta}_t) d\mathbf{z} = \nabla_{\boldsymbol{\theta}} \mathcal{L}_{\text{SGEM}}(\boldsymbol{\theta}) \Big|_{\boldsymbol{\theta}=\boldsymbol{\theta}_t}. \tag{37}$$

### B.3. Proof of Theorem 3.3

Assuming the E-step (9) is exact, we consider the second-order Taylor expansion of the M-step objective  $Q(\boldsymbol{\theta}|\boldsymbol{\theta}_t)$  (10)

$$\begin{aligned}
 Q(\boldsymbol{\theta}|\boldsymbol{\theta}_t) &\approx Q(\boldsymbol{\theta}_t|\boldsymbol{\theta}_t) \\
 &\quad + (\nabla_{\boldsymbol{\theta}} Q(\boldsymbol{\theta} \mid \boldsymbol{\theta}_t) \Big|_{\boldsymbol{\theta}=\boldsymbol{\theta}_t})^\top (\boldsymbol{\theta} - \boldsymbol{\theta}_t) \\
 &\quad + \frac{1}{2} (\boldsymbol{\theta} - \boldsymbol{\theta}_t)^\top (\nabla_{\boldsymbol{\theta}}^2 Q(\boldsymbol{\theta} \mid \boldsymbol{\theta}_t) \Big|_{\boldsymbol{\theta}=\boldsymbol{\theta}_t}) (\boldsymbol{\theta} - \boldsymbol{\theta}_t).
 \end{aligned} \tag{38}$$

Assuming the M-step (10) is also exact, the gradient of  $Q(\boldsymbol{\theta}|\boldsymbol{\theta}_t)$  at the maximum  $\boldsymbol{\theta}_{t+1}$  must be zero

$$\nabla_{\boldsymbol{\theta}} Q(\boldsymbol{\theta} \mid \boldsymbol{\theta}_t) \Big|_{\boldsymbol{\theta}=\boldsymbol{\theta}_{t+1}} = 0. \tag{39}$$

Replacing  $Q(\boldsymbol{\theta} \mid \boldsymbol{\theta}_t)$  with its the second-order Taylor approximation, we have

$$(\nabla_{\boldsymbol{\theta}} Q(\boldsymbol{\theta} \mid \boldsymbol{\theta}_t) \big|_{\boldsymbol{\theta}=\boldsymbol{\theta}_t}) + (\nabla_{\boldsymbol{\theta}}^2 Q(\boldsymbol{\theta} \mid \boldsymbol{\theta}_t) \big|_{\boldsymbol{\theta}=\boldsymbol{\theta}_t})(\boldsymbol{\theta}_{t+1} - \boldsymbol{\theta}_t) \approx 0. \quad (40)$$

Note that because

- $\nabla_{\boldsymbol{\theta}} \log p(\mathbf{x} \mid \boldsymbol{\theta}) \big|_{\boldsymbol{\theta}=\boldsymbol{\theta}_t} = \nabla_{\boldsymbol{\theta}} Q(\boldsymbol{\theta} \mid \boldsymbol{\theta}_t) \big|_{\boldsymbol{\theta}=\boldsymbol{\theta}_t}$  as shown in Theorem 3.1, and
- $\nabla_{\boldsymbol{\theta}}^2 Q(\boldsymbol{\theta} \mid \boldsymbol{\theta}_t) \big|_{\boldsymbol{\theta}=\boldsymbol{\theta}_t} = \mathbb{E}_{p(\mathbf{z} \mid \mathbf{x}; \boldsymbol{\theta}_t)} [\nabla_{\boldsymbol{\theta}}^2 \log p(\mathbf{x}, \mathbf{z} \mid \boldsymbol{\theta}_t)]$  by definition,

we can equivalently write as follows

$$\nabla_{\boldsymbol{\theta}} \log p(\mathbf{x} \mid \boldsymbol{\theta}_t) + \mathbb{E}_{p(\mathbf{z} \mid \mathbf{x}; \boldsymbol{\theta}_t)} [\nabla_{\boldsymbol{\theta}}^2 \log p(\mathbf{x}, \mathbf{z} \mid \boldsymbol{\theta}_t)] (\boldsymbol{\theta}_{t+1} - \boldsymbol{\theta}_t) = 0. \quad (41)$$

The term  $\mathbb{E}_{p(\mathbf{z} \mid \mathbf{x}; \boldsymbol{\theta}_t)} [\nabla_{\boldsymbol{\theta}}^2 \log p(\mathbf{x}, \mathbf{z} \mid \boldsymbol{\theta}_t)]$  is sometimes known as the *local* complete-data FIM. Simply taking the expectation on both sides w.r.t. a point mass  $p(\mathbf{x})$  over the observed data point  $\mathbf{x}$  yields

$$\nabla_{\boldsymbol{\theta}} \log p(\mathbf{x} \mid \boldsymbol{\theta}_t) + \underbrace{\mathbb{E}_{p(\mathbf{x}, \mathbf{z} \mid \boldsymbol{\theta}_t)} [\nabla_{\boldsymbol{\theta}}^2 \log p(\mathbf{x}, \mathbf{z} \mid \boldsymbol{\theta}_t)]}_{-\hat{F}(\boldsymbol{\theta}_t)} (\boldsymbol{\theta}_{t+1} - \boldsymbol{\theta}_t) = 0, \quad (42)$$

which can be rearranged as follows

$$\boldsymbol{\theta}_{t+1} = \boldsymbol{\theta}_t - \hat{F}(\boldsymbol{\theta}_t)^{-1} (-\nabla_{\boldsymbol{\theta}} \log p(\mathbf{x} \mid \boldsymbol{\theta}_t)). \quad (43)$$

#### B.4. Proof of Theorem 3.4

Assuming that the complete-data log-likelihood  $\log p(\mathbf{x}, \mathbf{z} \mid \boldsymbol{\theta})$  is twice differentiable, Lin et al. (2019) shows that generally the complete-data FIM  $\hat{F}(\boldsymbol{\theta})$  is block-diagonal.

In this section, we show that as a special case, a Gaussian mixture model  $p(\mathbf{x}, \mathbf{z} \mid \boldsymbol{\theta})$  with parameters  $\boldsymbol{\theta} = \{\boldsymbol{\pi}_k, \boldsymbol{\mu}_k, \boldsymbol{\Sigma}_k\}_{k=1}^K$  has a block-diagonal  $\hat{F}(\boldsymbol{\theta})$  with exactly  $K + 1$  blocks. We begin by writing down the complete-data log-likelihood

$$\log p(\mathbf{x}, \mathbf{z} \mid \boldsymbol{\theta}) = \sum_{k=1}^K \mathbb{1}_{\{\mathbf{z}=k\}} [\log \boldsymbol{\pi}_k + \log \mathcal{N}(\mathbf{x}; \boldsymbol{\mu}_k, \boldsymbol{\Sigma}_k)], \quad (44)$$

where  $\mathbb{1}_{\{\mathbf{z}=k\}}$  is the characteristic function that returns 1 when  $\mathbf{z} = k$  and 0 otherwise.

Note that  $\log p(\mathbf{x}, \mathbf{z} \mid \boldsymbol{\theta})$  can be equivalently rewritten as

$$\log p(\mathbf{x}, \mathbf{z} \mid \boldsymbol{\theta}) = \sum_{k=1}^K \mathbb{1}_{\{\mathbf{z}=k\}} \log \boldsymbol{\pi}_k + \sum_{k=1}^K \mathbb{1}_{\{\mathbf{z}=k\}} \log \mathcal{N}(\mathbf{x}; \boldsymbol{\mu}_k, \boldsymbol{\Sigma}_k) = \ell_{\boldsymbol{\pi}} + \sum_{k=1}^K \ell_k, \quad (45)$$

where  $\ell_{\boldsymbol{\pi}} = \sum_{k=1}^K \mathbb{1}_{\{\mathbf{z}=k\}} \log \boldsymbol{\pi}_k$  and  $\ell_k = \mathbb{1}_{\{\mathbf{z}=k\}} \log \mathcal{N}(\mathbf{x}; \boldsymbol{\mu}_k, \boldsymbol{\Sigma}_k)$ .

It is then clear that for any  $1 \leq i, j \leq K$  and  $i \neq j$ , we have

$$\nabla_{\boldsymbol{\mu}_i} \nabla_{\boldsymbol{\mu}_j} \log p(\mathbf{x}, \mathbf{z} \mid \boldsymbol{\theta}) = \nabla_{\boldsymbol{\mu}_i} \nabla_{\boldsymbol{\mu}_j} \ell_i = \mathbf{0}, \quad (46)$$

because  $\ell_i$  is a constant w.r.t.  $\boldsymbol{\mu}_j$ . Similarly, we can show that

$$\begin{aligned} \nabla_{\boldsymbol{\mu}_i} \nabla_{\boldsymbol{\mu}_j} \log p(\mathbf{x}, \mathbf{z} \mid \boldsymbol{\theta}) &= \nabla_{\boldsymbol{\mu}_i} \nabla_{\boldsymbol{\Sigma}_j} \log p(\mathbf{x}, \mathbf{z} \mid \boldsymbol{\theta}) = \\ \nabla_{\boldsymbol{\Sigma}_i} \nabla_{\boldsymbol{\mu}_j} \log p(\mathbf{x}, \mathbf{z} \mid \boldsymbol{\theta}) &= \nabla_{\boldsymbol{\Sigma}_i} \nabla_{\boldsymbol{\Sigma}_j} \log p(\mathbf{x}, \mathbf{z} \mid \boldsymbol{\theta}) = \\ \nabla_{\boldsymbol{\mu}_i} \nabla_{\boldsymbol{\pi}} \log p(\mathbf{x}, \mathbf{z} \mid \boldsymbol{\theta}) &= \nabla_{\boldsymbol{\Sigma}_i} \nabla_{\boldsymbol{\pi}} \log p(\mathbf{x}, \mathbf{z} \mid \boldsymbol{\theta}) = \\ \nabla_{\boldsymbol{\pi}} \nabla_{\boldsymbol{\mu}_j} \log p(\mathbf{x}, \mathbf{z} \mid \boldsymbol{\theta}) &= \nabla_{\boldsymbol{\pi}} \nabla_{\boldsymbol{\Sigma}_j} \log p(\mathbf{x}, \mathbf{z} \mid \boldsymbol{\theta}) = \mathbf{0}. \end{aligned} \quad (47)$$

Therefore, we can conclude that the Hessian of the complete-data log-likelihood is block-diagonal as all the off-diagonal blocks are zero matrices as we show above.

$$\nabla_{\boldsymbol{\theta}}^2 \log p(\mathbf{x}, \mathbf{z} | \boldsymbol{\theta}) = \begin{bmatrix} \nabla_{\boldsymbol{\mu}_1, \boldsymbol{\Sigma}_1}^2 \ell_1 & \cdots & 0 & 0 \\ \vdots & \ddots & \vdots & \vdots \\ 0 & \cdots & \nabla_{\boldsymbol{\mu}_K, \boldsymbol{\Sigma}_K}^2 \ell_K & \vdots \\ 0 & \cdots & \cdots & \nabla_{\boldsymbol{\pi}}^2 \ell_{\boldsymbol{\pi}} \end{bmatrix}. \quad (48)$$

Finally, note that by definition the complete-data FIM  $\hat{F}(\boldsymbol{\theta}) = -\mathbb{E}_{p(\mathbf{x}, \mathbf{z} | \boldsymbol{\theta})}[\nabla_{\boldsymbol{\theta}}^2 \log p(\mathbf{x}, \mathbf{z} | \boldsymbol{\theta})]$ , where

- The expectation of  $\nabla_{\boldsymbol{\mu}_k, \boldsymbol{\Sigma}_k}^2 \ell_k$  for  $k \in \{1, \dots, K\}$  is

$$\mathbb{E}_{p(\mathbf{x}, \mathbf{z} | \boldsymbol{\theta})}[\nabla_{\boldsymbol{\mu}_1, \boldsymbol{\Sigma}_1}^2 \ell_1] = \mathbb{E}_{p(\mathbf{z} | \boldsymbol{\theta})}[\mathbb{1}_{\{\mathbf{z}=k\}}] \cdot \mathbb{E}_{p(\mathbf{x} | \mathbf{z}; \boldsymbol{\theta})}[\nabla^2 \log \mathcal{N}(\mathbf{x}; \boldsymbol{\mu}_k, \boldsymbol{\Sigma}_k)] = \boldsymbol{\pi}_k \cdot -F_k, \quad (49)$$

- The expectation of  $\nabla_{\boldsymbol{\pi}}^2 \ell_{\boldsymbol{\pi}}$  is

$$\mathbb{E}_{p(\mathbf{x}, \mathbf{z} | \boldsymbol{\theta})}[\nabla_{\boldsymbol{\pi}}^2 \ell_{\boldsymbol{\pi}}] = \mathbb{E}_{p(\mathbf{x} | \mathbf{z}; \boldsymbol{\theta})} \mathbb{E}_{p(\mathbf{z} | \boldsymbol{\theta})}[\nabla^2 \log \text{Cat}(\mathbf{z}; \boldsymbol{\pi})] = -F_{\boldsymbol{\pi}}, \quad (50)$$

with  $F_k$  for  $k \in \{1, \dots, K\}$  being the FIM of the  $k$ -th Gaussian and  $F_{\boldsymbol{\pi}}$  being the FIM of the categorical distribution.

Therefore, the complete-data FIM  $\hat{F}(\boldsymbol{\theta})$  of a Gaussian mixture is given as follows

$$\hat{F}(\boldsymbol{\theta}) = -\mathbb{E}_{p(\mathbf{x}, \mathbf{z} | \boldsymbol{\theta})}[\nabla_{\boldsymbol{\theta}}^2 \log p(\mathbf{x}, \mathbf{z} | \boldsymbol{\theta})] = \begin{bmatrix} \boldsymbol{\pi}_1 F_1 & \cdots & 0 & 0 \\ \vdots & \ddots & \vdots & \vdots \\ 0 & \cdots & \boldsymbol{\pi}_K F_K & \vdots \\ 0 & \cdots & \cdots & F_{\boldsymbol{\pi}} \end{bmatrix}. \quad (51)$$

## B.5. Fisher Information Matrix of Gaussian Mixtures

Consider a Gaussian mixture model with parameters  $\boldsymbol{\theta} = \{\boldsymbol{\pi}_k, \boldsymbol{\mu}_k, \boldsymbol{\Sigma}_k\}_{k=1}^K$ . The log density is

$$\log p(\mathbf{x} | \boldsymbol{\theta}) = \log \sum_{k=1}^K \boldsymbol{\pi}_k \mathcal{N}(\mathbf{x}; \boldsymbol{\mu}_k, \boldsymbol{\Sigma}_k). \quad (52)$$

The gradient of the log density is

$$\nabla_{\boldsymbol{\theta}} \log p(\mathbf{x} | \boldsymbol{\theta}) = \frac{\sum_{k=1}^K \nabla_{\boldsymbol{\theta}} [\boldsymbol{\pi}_k \mathcal{N}(\mathbf{x}; \boldsymbol{\mu}_k, \boldsymbol{\Sigma}_k)]}{\sum_{k=1}^K \boldsymbol{\pi}_k \mathcal{N}(\mathbf{x}; \boldsymbol{\mu}_k, \boldsymbol{\Sigma}_k)}. \quad (53)$$

We can see that the gradient w.r.t. any parameter will also depend on all other parameters through the denominator term  $\sum_{k=1}^K \boldsymbol{\pi}_k \mathcal{N}(\mathbf{x}; \boldsymbol{\mu}_k, \boldsymbol{\Sigma}_k)$ , which is not factorizable due to the log-sum term in  $\log p(\mathbf{x} | \boldsymbol{\theta})$ .

The interdependence structure of the log density gradient results in highly complex Hessian matrices, which is often undesirable and practically intractable to evaluate. Furthermore, one needs to compute the FIM (negative expected Hessian) via numerical integration, which exacerbates the intractability.

## B.6. Fisher Information Matrix of Gaussian Distributions

Consider a Gaussian distribution with parameters  $\boldsymbol{\theta} = \{\boldsymbol{\mu}, \boldsymbol{\sigma}\}$ . The log density is

$$\log p(\mathbf{x} | \boldsymbol{\theta}) = -\log \det(\text{diag}(\boldsymbol{\sigma})) - \frac{1}{2} (\mathbf{x} - \boldsymbol{\mu})^\top \text{diag}(\boldsymbol{\sigma}^{-2}) (\mathbf{x} - \boldsymbol{\mu}). \quad (54)$$

The gradient of the log density is

$$\nabla_{\boldsymbol{\mu}} \log p(\mathbf{x}|\boldsymbol{\theta}) = \frac{\mathbf{x} - \boldsymbol{\mu}}{\sigma^2}, \quad (55)$$

$$\nabla_{\sigma} \log p(\mathbf{x}|\boldsymbol{\theta}) = \frac{(\mathbf{x} - \boldsymbol{\mu})^2}{\sigma^3} - \frac{1}{\sigma}. \quad (56)$$

The Hessian of the log density is

$$\nabla_{\boldsymbol{\mu}} \nabla_{\boldsymbol{\mu}} \log p(\mathbf{x}|\boldsymbol{\theta}) = -\frac{1}{\sigma^2}, \quad (57)$$

$$\nabla_{\boldsymbol{\mu}} \nabla_{\sigma} \log p(\mathbf{x}|\boldsymbol{\theta}) = -\frac{2(\mathbf{x} - \boldsymbol{\mu})}{\sigma^3}, \quad (58)$$

$$\nabla_{\sigma} \nabla_{\boldsymbol{\mu}} \log p(\mathbf{x}|\boldsymbol{\theta}) = -\frac{2(\mathbf{x} - \boldsymbol{\mu})}{\sigma^3}, \quad (59)$$

$$\nabla_{\sigma} \nabla_{\sigma} \log p(\mathbf{x}|\boldsymbol{\theta}) = -\frac{3(\mathbf{x} - \boldsymbol{\mu})^2}{\sigma^4} + \frac{1}{\sigma^2}. \quad (60)$$

Note that because  $\mathbb{E}_{p(\mathbf{x}|\boldsymbol{\theta})}[\mathbf{x} - \boldsymbol{\mu}] = 0$  and  $\mathbb{E}_{p(\mathbf{x}|\boldsymbol{\theta})}[(\mathbf{x} - \boldsymbol{\mu})^2] = \sigma^2$ , we can derive that

$$F([\boldsymbol{\mu} \ \boldsymbol{\sigma}]) = -\mathbb{E}_{p(\mathbf{x}|\boldsymbol{\theta})} \begin{bmatrix} \nabla_{\boldsymbol{\mu}} \nabla_{\boldsymbol{\mu}} \log p(\mathbf{x}|\boldsymbol{\theta}) & \nabla_{\boldsymbol{\mu}} \nabla_{\sigma} \log p(\mathbf{x}|\boldsymbol{\theta}) \\ \nabla_{\sigma} \nabla_{\boldsymbol{\mu}} \log p(\mathbf{x}|\boldsymbol{\theta}) & \nabla_{\sigma} \nabla_{\sigma} \log p(\mathbf{x}|\boldsymbol{\theta}) \end{bmatrix} = \begin{bmatrix} \frac{1}{\sigma^2} & 0 \\ 0 & \frac{2}{\sigma^2} \end{bmatrix}. \quad (61)$$

## B.7. Fisher Information Matrix of Categorical Distributions

Consider a categorical distribution parametrized by logits  $\boldsymbol{\psi}$  such that the probabilities  $\boldsymbol{\pi} = \text{softmax}(\boldsymbol{\psi})$ . Let  $\mathbf{x}$  be a one-hot vector describing the event outcome. The log density is

$$\log p(\mathbf{x}|\boldsymbol{\psi}) = \mathbf{x}^\top \boldsymbol{\psi} - \log \sum_k \exp(\psi_k). \quad (62)$$

The gradient of the log-density is

$$\nabla_{\boldsymbol{\psi}} \log p(\mathbf{x}|\boldsymbol{\theta}) = \mathbf{x} - \boldsymbol{\pi}. \quad (63)$$

The Hessian of the log-density (for  $i \neq j$ ) is

$$\nabla_{\psi_i} \nabla_{\psi_j} \log p(\mathbf{x}|\boldsymbol{\theta}) = -\nabla_{\psi_j} \boldsymbol{\pi}_i = \boldsymbol{\pi}_i \boldsymbol{\pi}_j, \quad (64)$$

$$\nabla_{\psi_i} \nabla_{\psi_i} \log p(\mathbf{x}|\boldsymbol{\theta}) = -\nabla_{\psi_i} \boldsymbol{\pi}_i = \boldsymbol{\pi}_i^2 - \boldsymbol{\pi}_i. \quad (65)$$

Putting together in matrix form, the Hessian  $\nabla^2 \log p(\mathbf{x}|\boldsymbol{\psi}) = \boldsymbol{\pi} \boldsymbol{\pi}^\top - \text{diag}(\boldsymbol{\pi})$ . Therefore, we can derive the FIM

$$F(\boldsymbol{\psi}) = -\mathbb{E}_{p(\mathbf{x}|\boldsymbol{\psi})}[\nabla^2 \log p(\mathbf{x}|\boldsymbol{\psi})] = \text{diag}(\boldsymbol{\pi}) - \boldsymbol{\pi} \boldsymbol{\pi}^\top. \quad (66)$$

However, note that under this parametrization, the FIM  $F(\boldsymbol{\psi})$  is not invertible (one can verify that  $F(\boldsymbol{\psi})\mathbf{1} = 0$ ). Instead, we replace the inverse of  $F(\boldsymbol{\psi})$  with the Moore-Penrose pseudo-inverse in practice

$$F(\boldsymbol{\psi})^+ = \text{diag}(\boldsymbol{\pi})^{-1} - \mathbf{1}\mathbf{1}^\top. \quad (67)$$

Therefore, the complete-data natural gradient  $\hat{\nabla}_{\boldsymbol{\psi}}$  w.r.t. the logits  $\boldsymbol{\psi}$  can be simplified to

$$\begin{aligned} \hat{\nabla}_{\boldsymbol{\psi}} &= F(\boldsymbol{\psi})^+ \nabla_{\boldsymbol{\psi}} \log p(\mathbf{x}|\boldsymbol{\theta}) \\ &= (\text{diag}(\boldsymbol{\pi})^{-1} - \mathbf{1}\mathbf{1}^\top)(\mathbf{x} - \boldsymbol{\pi}) \\ &= \text{diag}(\boldsymbol{\pi})^{-1} \mathbf{x} - \mathbf{1}. \end{aligned} \quad (68)$$

## C. Implementation

We provide a reference implementation of our approach using the JAX (Bradbury et al., 2018) framework.

```

import jax
from jax.numpy import jnp

Dist = tuple["weight", "mu", "sigma"]

def mdn(x) -> Dist:
    ...

@jax.custom_jvp
def precond(dist: Dist) -> Dist:
    return dist

@precond.defjvp
def _(primals, tangents):
    dist, grads = *primals, *tangents
    d_w, d_mu, d_sigma = dist
    g_w, g_mu, g_sigma = grads
    return dist, (g_w, g_mu * d_std ** 2, g_std / 2.0 * d_std ** 2)

def ngem_loss(x, y):
    d_w, d_mu, d_sigma = jax.vmap(mdn)(x)
    # Apply natural gradient preconditioning
    d_w, d_mu, d_sigma = precond((d_w, d_mu, d_sigma))
    # [E-step] compute responsibilities rho
    log_weights = jax.nn.log_softmax(d_w, axis=-1)
    # Standard Gaussian log probability for each component
    log_normal = jax.vmap(gaussian_log_prob)(d_mu, d_sigma, y[:, jnp.newaxis])
    log_rho = jax.nn.log_softmax(log_weights + log_normal, axis=-1)
    rho = jax.lax.stop_gradient(jnp.exp(log_rho))
    # [M-step] natural gradient descent
    pi = jax.lax.stop_gradient(jnp.exp(log_weights))
    return -(rho / pi * (log_weights + log_normal)).sum(axis=-1).mean()

```

## D. Experiments

We provide additional experiment details in this section. All experiments are conducted on a RTX 4090 GPU workstation.

### D.1. Hyperparameters

Tables 7 to 9 reports the hyperparameter settings for all experiments discussed in Section 4.

Table 7. Hyperparameter settings for Two-Gaussians experiments.

Hyperparameter	Value
Number of Components ( $K$ )	2
Optimizer	SGD
Learning Rate ( $\beta$ )	$\{10^{-1}, 10^{-2}, 10^{-3}\}$
Epochs	50
Batch Size	1
Dataset Size	200 ( $2 \times 100$ )
Random Seeds	$\{1, 2, 3, 4, 5\}$

Table 8. Hyperparameter settings for Two-Sinusoids experiments.

Hyperparameter	Value
Number of Components ( $K$ )	2
Hidden Layer Sizes	[128, 128, 128, 128]
Activation Function	GELU (Hendrycks & Gimpel, 2023)
Optimizer	Adam
Learning Rate ( $\beta$ )	$\{10^{-3}, 10^{-4}, 10^{-5}\}$
Epochs	1000
Batch Size	128
Dataset Size	2000 ( $2 \times 1000$ )
Random Seeds	$\{1, 2, 3, 4, 5\}$

Table 9. Hyperparameter settings for inverse-MNIST experiments.

Hyperparameter	Value
Number of Components ( $K$ )	$\{3, 10, 20\}$
Hidden Layer Sizes	[128, 128, 128, 128]
Activation Function	GELU (Hendrycks & Gimpel, 2023)
Optimizer	Adam
Learning Rate ( $\beta$ )	$3 \times 10^{-4}$
Epochs	100
Batch Size	256
Dataset Size	60000
Random Seeds	$\{1, 2, 3, 4, 5\}$

Table 10. Hyperparameter settings for {kin8nm, energy, housing} experiments.

Hyperparameter	Value
Number of Components ( $K$ )	3
Hidden Layer Sizes	[128, 128]
Activation Function	GELU (Hendrycks & Gimpel, 2023)
Optimizer	{Adam, KFAC, Muon, Soap}
Learning Rate ( $\beta$ )	{kin8nm: $10^{-3}$ , others: $10^{-4}$ }
Epochs	{kin8nm: 250, others: 125}
Batch Size	{kin8nm: 128, energy: 16, housing: 32}
Dataset Size	{kin8nm: 8192, energy: 768, housing: 506}
Random Seeds	$\{1, 2, 3, 4, 5\}$

## D.2. Inverse-MNIST

Figures 9 and 10 illustrates the Gaussian mixture ( $K = 3$ ) component means predicted by mixture density networks, trained using either nGEM (Figure 9) or NLL (Figure 10). We can observe that nGEM predicts sharp and diverse images, while NLL predicts blurry, visually similar images, and suffers from mode collapse (some  $\pi_k = 1$  for all classes).

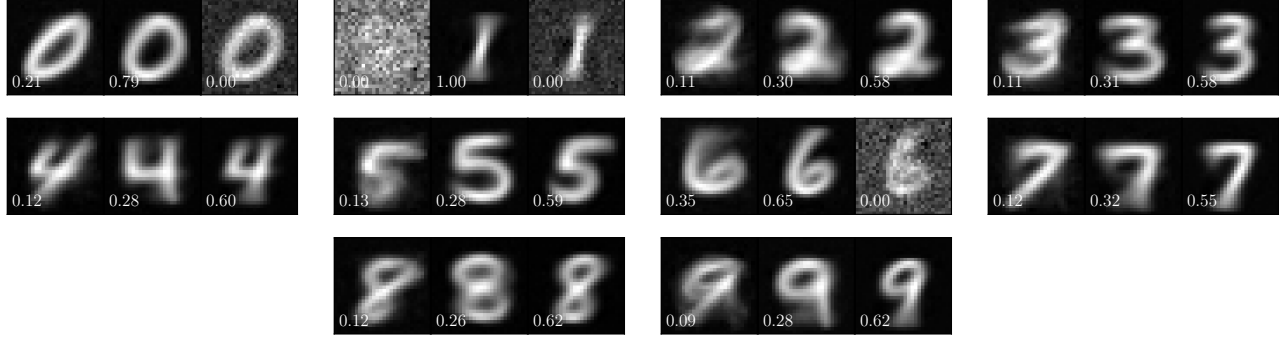


Figure 9. (nGEM) Visualizing the predicted Gaussian mixture ( $K = 3$ ) component means  $\mu_k$  given class labels  $\{0, 1, \dots, 9\}$  for the inverse-MNIST example. Numbers to the bottom left corner of each image denote the corresponding mixture component weight  $\pi_k$ .

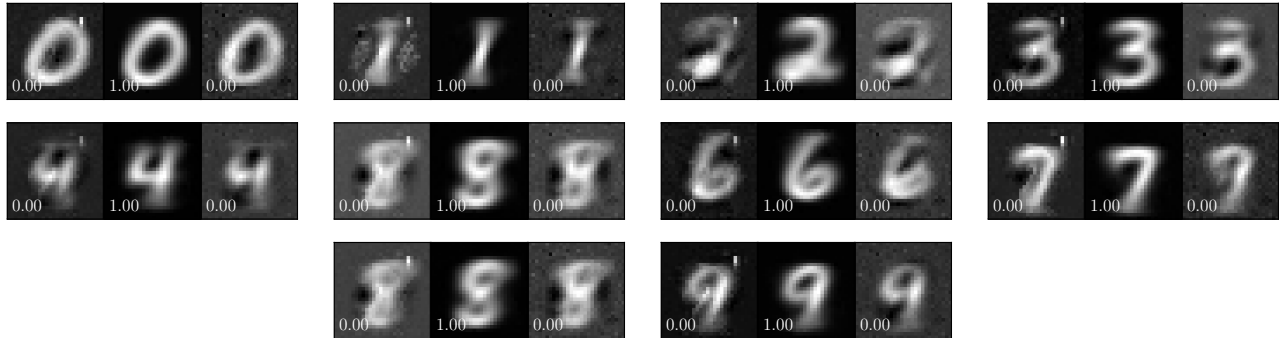


Figure 10. (nLL) Visualizing the predicted Gaussian mixture ( $K = 3$ ) component means  $\mu_k$  given class labels  $\{0, 1, \dots, 9\}$  for the inverse-MNIST example. Numbers to the bottom left corner of each image denote the corresponding mixture component weight  $\pi_k$ .